european corporate governance institute

Biodiversity Impacts of Renewable Energy

Finance Working Paper N° 1111/2025
Revised May 2026

Haozhou Gong
The University of Hong Kong
Chen Lin
The University of Hong Kong
Zacharias Sautner
University of Zurich, Swiss Finance Institute and ECGI
Thomas Schmid
The University of Hong Kong

© Haozhou Gong, Chen Lin, Zacharias Sautner and Thomas Schmid 2026. All rights reserved. Short sections of text, not to exceed two paragraphs, may be quoted without explicit permission provided that full credit, including © notice, is given to the source.

This paper can be downloaded without charge from:
https://doi.org/10.67929/ecgi-fin-1111-2025

european corporate governance institute

ECGI Working Paper Series in Finance

Biodiversity Impacts of Renewable Energy

Working Paper N° 1111/2025

May 2026

Haozhou Gong
Chen Lin
Zacharias Sautner
Thomas Schmid

We are very grateful to Haotian Feng for outstanding research assistance. We also thank Jie-Sheng Tan-Soo, Arthur van Benthem, seminar participants at the Academy of Mathematics and Systems Science of the Chinese Academy of Sciences, and conference participants at the 2026 SGFIN Research Conference in Singapore and the 2026 UNC Energy Finance and Climate Transition Risk conference in Chapel Hill. Sautner is on the Sustainability Council of Lampe Asset Management.

© Haozhou Gong, Chen Lin, Zacharias Sautner and Thomas Schmid 2025. All rights reserved. Short sections of text, not to exceed two paragraphs, may be quoted without explicit permission provided that full credit, including © notice, is given to the source.

Abstract

Renewable energy is essential for mitigating climate change but can harm biodiversity through habitat loss. We combine spatial biodiversity data, satellite imagery, and asset-level information on 47,616 hydro, solar, and wind plants to construct a measure of their biodiversity impacts. Solar plants have high aggregate impacts due to land use, while hydro plants are often sited in biodiversity-sensitive areas. Impacts are highly concentrated, skewed, and vary across plants by owner type (listed versus unlisted, financial versus non-financial) and f inancing structure (project versus corporate finance). Counterfactual analyses show that nearby siting alternatives could reduce impacts substantially without foregoing renewable energy investment.

Keywords: Renewable energy, Biodiversity risk, Nature risk

Haozhou Gong
Researcher
The University of Hong Kong
12/F, Cheng Yu Tung Building
Hong Kong, China
e-mail: gonghz@connect.hku.hk

Chen Lin
Stelux Professor in Finance
The University of Hong Kong
K. K. Leung Building, Pok Fu Lam Road
Hong Kong, China
e-mail: chenlin1@hku.hk

Zacharias Sautner*
Professor of Sustainable Finance
University of Zurich
Plattenstrasse 14
CH-8032 Zurich, Switzerland
e-mail: zacharias.sautner@bf.uzh.ch

Thomas Schmid
Associate Professor of Finance
The University of Hong Kong
K. K. Leung Building, Pok Fu Lam Road
Hong Kong, China
e-mail: schmid@hku.hk

*Corresponding Author

Biodiversity Impacts of Renewable Energy

Haozhou Gong, Chen Lin, Zacharias Sautner, Thomas Schmid*

May 22, 2026

ABSTRACT

Renewable energy is essential for mitigating climate change but can harm biodiversity through habitat loss. We combine spatial biodiversity data, satellite imagery, and asset-level information on 47,616 hydro, solar, and wind plants to construct a measure of their biodiversity impacts. Solar plants have high aggregate impacts due to land use, while hydro plants are often sited in biodiversity-sensitive areas. Impacts are highly concentrated, skewed, and vary across plants by owner type (listed versus unlisted, financial versus non-financial) and financing structure (project versus corporate finance). Counterfactual analyses show that nearby siting alternatives could reduce impacts substantially without foregoing renewable energy investment.

*Haozhou Gong, Chen Lin, and Thomas Schmid (corresponding author, schmid@hku.hk) are at the University of Hong Kong. Zacharias Sautner is at the University of Zurich and the Swiss Finance Institute. We are very grateful to Haotian Feng for outstanding research assistance. We also thank Jie-Sheng Tan-Soo, Arthur van Benthem, seminar participants at the Academy of Mathematics and Systems Science of the Chinese Academy of Sciences, and conference participants at the 2026 SGFIN Research Conference in Singapore and the 2026 UNC Energy Finance and Climate Transition Risk conference in Chapel Hill. Sautner is on the Sustainability Council of Lampe Asset Management.

Transitioning towards renewable energy (RE) is the central pillar of climate change mitigation. According to estimates, investments in RE need to more than double from $624 billion in 2024 to $1.4 trillion per year over the 2025-2030 period to meet globally agreed-upon climate targets (IRENA, 2025). Parts of the RE demand are due to the AI boom, which requires massive amounts of electricity to power data centers, and many AI companies have made commitments to use renewable sources to meet their energy needs (e.g., Nvidia, 2025). Yet, this transition can generate significant and underexamined tradeoffs with biodiversity conservation because RE investments can involve environmental costs if solar, hydro, or wind plants destroy habitats or fragment ecosystems through infrastructure. In other words, although RE is beneficial for the environment, careful consideration must be given to the siting of RE plants to ensure that efforts to address climate change do not generate unintended consequences for biodiversity.[1]

The biodiversity impacts of RE can be financially material for investors and firms. Giglio et al. (2026b) document that RE producers are among the most frequent disclosers of biodiversity-related risks in their Form 10-K annual reports. With RE producers and investors becoming increasingly aware of their potential biodiversity impacts, some are actively considering ways to address them in their decision-making.[2] Evidence also suggests that the interactions between addressing climate change and biodiversity loss are beginning to be reflected in asset prices: Stroebel and Zeng (2025) document that RE projects aimed at hedging investor portfolios against climate transition risks simultaneously expose investors to biodiversity risks.

How the tradeoffs between RE and biodiversity loss are identified, measured, and managed is therefore a fundamental question, particularly for finance, which plays a critical role in allocating capital and shaping the design of RE projects. Notably, investors, firms, and their regulators increasingly rely on environmental metrics, risk assessments, and sustainability frameworks to evaluate RE investments, but these tools often prioritize carbon reduction while insufficiently accounting for biodiversity impacts. Understanding how finance can evaluate and mitigate the climate–biodiversity tradeoff is therefore important for assessing whether capital allocation mecha-

[1] Transition-related tradeoffs exist in other areas too, for example if the surge in the surface-mining of raw materials for electric vehicles or batteries destroys forests and habitats.

[2] Asset manager NextEnergy Group, for example, which focuses on the development, operation and financing of RE assets, has developed a nature strategy that includes the commitment that their investments do not contribute to the conversion of natural ecosystems (NextEnergy, 2025).

nisms promote truly sustainable outcomes or instead shift environmental risks across dimensions.

Despite the fundamental importance of this topic, large-scale, comprehensive evidence on the biodiversity impacts of RE is lacking, largely because of measurement challenges. Existing studies are either geographically limited or lack a standardized measurement of biodiversity impacts, which constrains the comparability of any results across regions, technologies, or time. We make significant progress in addressing these challenges by constructing a novel global measure of the land-use-induced biodiversity impacts of RE plants, combining spatial biodiversity data, satellite imagery, and asset-level information on power plants.[3] Using this measure, we make three key contributions. First, we quantify the biodiversity impacts of existing RE plants and analyze how scenarios for RE expansion are expected to affect biodiversity. Second, we document that the biodiversity impact of RE is concentrated among a small number of plants and quantify how much it could be reduced if high-impact solar and wind plants were instead sited in nearby alternative locations. Third, we shed light on how biodiversity impacts vary across the firms behind RE plants and across the financing structures of the RE plants themselves.

To measure land-use-induced biodiversity impact, we rely on the Species Threat Abatement and Restoration (STAR) score developed by Mair et al. (2021). This score is a key metric proposed by the Taskforce on Nature-related Financial Disclosures (TNFD) and the Finance for Biodiversity Foundation to quantify biodiversity impacts, and is ranked among the biodiversity risk metrics for investors and firms with the highest scientific grounding (Kashyap et al., 2025). We employ specifically the Threat Abatement STAR (STAR_T) subscore, which quantifies at a granular 5 by 5 km^2 level how much extinction risk could be reduced if current threats were removed. This enables us to quantify the biodiversity impact that could have been avoided had a RE plant not been built. High STAR_T scores in an area indicate locations with many threatened species, a large proportion of individual species' ranges, or species that are severely threatened.[4]

We combine STAR_T data with information on 47,616 solar, wind, and hydro plant units from around the world with a capacity of at least one megawatt (MW) constructed between 2000

[3]Land use constitutes the single most important channel through which business activities negatively impact biodiversity, ahead of greenhouse gas emissions, water pollution, or toxic emissions (Díaz et al., 2019).

[4]Two other biodiversity footprinting metrics proposed by the Finance for Biodiversity Foundation are Mean Species Abundance (MSA) and Potentially Disappeared Fraction of Species (PDF). These measures are used by data vendors such as MSCI, ISS or Iceberg Data Lab but do not build on spatial data.

and 2025. The capacity of these plants is 1.61 terawatts (TW), exceeding today's 1.30 TW electricity generation capacity in the U.S. We identify the exact location of power plants, calculate their land use with remote sensing data or capacity-based approximations, and spatially match their land-use footprints with STAR_T data. Our satellite imagery–based approach enables us to quantify the biodiversity impact of each plant by measuring the exact overlap between plant footprints and species' habitats. This approach offers advantages over relying solely on point coordinates, which often indicate administrative or office locations and reveal little about a plant's spatial extent—imagery data instead allow us to track the true plant footprint, to distinguish multi-unit clusters, and to allocate area across adjacent plants. Furthermore, time-stamped satellite imagery enables us to verify that land conversion coincides with construction, to exclude pre-existing built-up areas from biodiversity calculations, and to capture before–after changes such as reservoir inundation for hydropower.[5] This substantially reduces measurement error in siting and land-use attribution compared to coordinate-only methods. By providing a verifiable biodiversity impact measurement, our asset-level approach complements estimation- or disclosure-based approaches (Garel et al., 2024; Giglio et al., 2026b).

Our first contribution, the quantification exercise, shows that RE plants generate an aggregate biodiversity impact, calculated as the total STAR_T score across all plants, of about 5 billion, which is equivalent to the value of the entire forested area in Austria. To substantiate our measurements, given that STAR_T scores are abstract, we use IUCN Red List data to demonstrate that RE plants impact a substantial number of vulnerable and critically endangered species. We further show that it is crucial to differentiate RE technologies when evaluating climate-biodiversity tradeoffs. Solar and hydro account for nearly 90% of the overall biodiversity impact, whereas wind contributes relatively little. Solar plants have a large impact due to their large land requirements—imposing the highest total land use across all technologies—whereas the impact of hydro plants arises primarily because such facilities are disproportionately sited in biodiversity-sensitive locations. These conclusions are unaffected if we scale biodiversity impacts by a plant's expected generation capacity. The temporal dimensions of biodiversity impacts are

[5]The high-frequency, long-run archival data that we employ also helps filter problematic observations, such as misrecorded office coordinates, misgeolocations on water or in dense settlements, and helps identify plants built on already developed land (with near-zero biodiversity value).

equally striking. Over the past two decades, biodiversity impacts linked to RE expansion have risen sharply, largely because of rising land use per project, rather than siting in more sensitive locations. Solar has overtaken hydro as the dominant impact driver in the last decade.

A key question is how the biodiversity impact of RE is expected to evolve in the years ahead. This assessment is important given the massive projected growth in RE capacity.[6] When considering, on top of existing plants, those under construction or planned, RE's biodiversity impact increases by 50%, from a STAR_T score of 5 billion to 7.5 billion. This number is equivalent to the value of the entire land area in Senegal, a biodiversity heaven known for its species richness. If we alternatively quantify impacts based on projected growth figures until 2030 by the International Energy Agency (IEA), we calculate a STAR_T value of twice that number (14 billion) by 2030 (IEA, 2026) (the IEA's projections include also non-planned projects). Using long-term projections about RE generation by 2050 (IEA, 2025), the STAR_T score could increase to 53 billion, equivalent to the biodiversity value of the entire land area in Canada or Uganda. Our approach is therefore not only relevant in quantifying the impact of existing RE plants, but can also be used when evaluating future projects.

In our second contribution, we document that RE's biodiversity impacts are heterogeneous and highly skewed because a small number of projects have exceptionally large impacts. We calculate that fewer than 1% of all plants account for nearly 70% of the overall biodiversity impact, but provide less than 5% of the generation capacity. Given this concentration, we analyze how much the biodiversity impact could be reduced if these high-impact plants had hypothetically been sited in realistic counterfactual areas with the lowest-possible biodiversity value within a specific radius around their locations (excluding locations where alternative siting would be impossible). Focusing on solar and wind, given that hydro projects are tied to specific locations, we quantify that the impact of the worst 1% of plants could be reduced by more than 90% even within a radius of only 10 kilometers. This implies that targeted siting policies, combined with stricter biodiversity safeguards, could have substantially reduced environmental costs without

[6] In fact, about 80% of the projected capacity growth will come from solar (IEA, 2024), which currently accounts for about half of the total impact of RE. Also on the hydro side, a surge in new projects is projected and studies estimate that at least 3,700 major dams are planned or under construction (Zarfl et al., 2015); this growth primarily comes from emerging economies, including many biodiversity-rich ones.

constraining capacity growth.[7]

For our third contribution, we examine the heterogeneity of biodiversity impacts across the firms behind RE projects (e.g., utilities or developers). Consistent with our plant-level evidence, firm-level biodiversity impacts are also highly concentrated and skewed, even among firms using the same generation technology within narrowly defined regions. For investors, this demonstrates that they can significantly reduce biodiversity risk in their portfolios simply by avoiding the worst-performing firms, without reducing their investments in RE. For time-constrained regulators, this heavy concentration implies that focusing attention on the few firms responsible for the most severe damage maximizes regulatory effectiveness.

We build on this insight by examining differences in ownership and financing structures across plants. While none of these tests are intended to establish a causal relationship, they highlight important financial factors associated with the impact of RE plants. The first analysis shows that plants owned by listed firms have a two-thirds higher biodiversity impact compared to plants of unlisted firms with the same generation technology located in the same narrowly-defined region. However, after controlling for a plant's expected electricity generation, the difference disappears. This, together with similar impacts per unit of generation and land use across both groups, suggests that differences between listed and unlisted firms mainly reflect scale effects from larger publicly owned plants. However, when comparing listed and unlisted firms *within* the same ultimate parent company, we find consistently that plants of listed firms have a lower impact, even after accounting for generation capacity differences. That parent firms place high-impact plants in unlisted subsidiaries is consistent with listed subsidiaries facing greater environmental scrutiny from investors, regulators, and the public (Duchin, Gao, and Xu, 2025).

The second analysis shows that plants owned by financial firms have a 10% lower biodiversity impact compared to those of non-financial firms, even after controlling for expected generation. In terms of siting decisions, there is also evidence that plants of financial firms locate in less biodiversity-sensitive areas. These results are similar when we compare plants from financial and non-financial firms within the same ultimate parent company. One explanation is that

[7] An example is the Ichigo Nago Futami Eco Power Plant in Japan, for which we show that a counterfactual siting just 9.2 km away would have reduced the plant's impact by 98%.

financial institutions—as argued in the prior literature—face relatively stronger ESG-related financial, reputational, and normative pressures. Hence, they may have become more attentive to the biodiversity risks of their investments.

The third analysis finds that project-financed plants (via ring-fenced Special Purpose Vehicles) exhibit systematically higher biodiversity impacts compared to plants financed directly on corporate balance sheets. This difference remains robust, and strengthens in magnitude, when comparing project-financed and corporate-financed plants within the same ultimate parent company. This suggests that firms are reluctant to hold biodiversity risks on their balance sheets, for example because of heightened scrutiny from investors, regulators, or the public.[8]

Existing studies regarding the biodiversity impacts of RE are highly fragmented, either focusing on single technologies, case studies, or country-level approximations.[9] While insightful, the existing evidence is either geographically limited, lacks project-level information, or does not apply standardized measures of biodiversity impact, constraining the ability to assess the biodiversity impact of RE across regions, technologies, and time. Thus, a systematic global quantification of the biodiversity impact of RE plants remains absent. We make significant progress along all of these dimensions by providing a comprehensive, global assessment of the impact of RE using a standardized biodiversity metric that is comparable across regions, technologies, and time.

We also contribute to a growing body of work in economics and finance that focuses on biodiversity. Flammer, Giroux, and Heal (2025) show that blended instruments can mobilize private investment for conservation, Giglio et al. (2026b) and Garel et al. (2024) document that biodiversity risks already affect equity prices, and Chen et al. (2025) find that stricter enforcement of biodiversity conservation in China raised municipal borrowing costs. Frank and

[8]While initiatives such as the Equator Principles aim to enhance environmental due diligence for capital providers of project finance, their effect thus far appears limited (Berg et al., 2025).

[9]For solar plants, studies show that large-scale solar PV installations are disproportionately sited in shrublands, scrublands, croplands, and grasslands, which often overlap with sensitive habitats (Hernandez et al., 2015; Kruitwagen et al., 2021). Regional studies confirm negative outcomes for wildlife; for instance, bird species richness and density decline close to PV facilities in South Africa (Visser et al., 2019). Garrett and Shive (2026) examine the link between solar plant siting in the U.S. and the presence of endangered species. For wind plants, Cryan et al. (2014) demonstrate high bat fatality rates near wind turbines, and Thaker, Zambre, and Bhosale (2018) and Meng et al. (2025) show that wind farms reduce bird abundance in India and China, potentially triggering cascading trophic effects such as shifts in lizard populations. Wang et al. (2025) evaluate the RE-related biodiversity loss using a countryside species-area relationship model. However, their study ends in 2015 and relies on national averages rather than project-level information. See Gasparatos et al. (2017) for a more comprehensive review of this literature.

Sudarshan (2024) quantify the social costs of species collapse. We contribute to this literature by providing an evaluation of the relationship between RE plants' ownership/financing and their biodiversity impact. More broadly, we complement this literature by introducing a novel approach to measuring the biodiversity impact of firms at the asset level. When combined with improved access to asset-level data beyond the electricity generation sector in the future, this method has the potential to address the current challenges in accurately assessing location-based biodiversity risk exposures. Such advancements can significantly advance research in this area, which has been limited by measurement difficulties as emphasized by Giglio et al. (2026a). Moving forward, our approach can be applied to manufacturing plants, data centers, or other infrastructure projects. Currently, this is not possible at scale as most firms do not report on their asset locations. However, with new nature-related disclosure requirements developed by standard setters such as the International Accounting Standards Board, the lack of location data will change in the near future. Our paper can also function as an illustration of how biodiversity impacts can be quantified for corporate reporting.

1. Data

This section describes the data we use to measure the biodiversity impacts of RE plants.

1.1 Power Plant Data

We create a sample of RE plants using the S&P Market Intelligence (S&P MI) database, which provides comprehensive global coverage for power plant units with a capacity of at least 1 MW. For simplicity, we refer to plant *units* as *plants* (unless it is important to distinguish between the two).[10] The dataset includes information on a plant unit's geographic coordinates (latitude/longitude), generation technology, operational status and start of commercial operations, generation capacity, equipment details, and direct as well as ultimate owners.

We apply several data filters for plant units to end up in our sample. First, for the scope of this study, RE includes solar photovoltaic, concentrated solar power, wind farms, and hy-

[10] Most plants consist of one plant unit but there are cases where one plant has multiple units, which can differ, for example, in their generation technologies.

dropower facilities (including pumped storage); we omit a few RE technologies that play only a modest role for energy production today (e.g., geothermal plants). Second, we exclude 193 power plant units for which the coordinates in S&P MI are located on water (offshore wind farms), because no comprehensive data exist to assess underwater biodiversity impacts; these restrictions apply to measuring both ocean biodiversity in general, and to the specific biodiversity metric we employ (Mair et al., 2021). Third, we exclude 2,504 plant units whose geographic coordinates are missing or incorrect (based on manual verification of satellite images). Fourth, we focus on power plant units that became operational between 2000 and 2025. This implies in particular that we do not consider hydro capacity built before 2000.

Our final dataset covers 47,616 RE plant units across 190 countries, consisting of 13,556 hydro, 17,715 solar, and 16,345 wind units. These plants have a total capacity of about 1.61 TW, roughly 95% of the total utility-scale RE capacity in S&P MI by 2025.[11]

Figure 1 illustrates the locations of the sampled solar, wind, and hydro plants, showing that RE plants are concentrated most densely in North America, Europe, and East Asia, and that the three technologies exhibit distinct spatial patterns. Figure 2 visualizes the evolution of RE plants over time. Panel (a) reports the yearly number of newly installed plants. In the early sample years, wind and hydro were the most common technologies, while solar has become more common since the 2010s. Solar overtook wind and hydro around 2015. New RE plants reached a peak in 2015 and declined substantially afterwards. Panel (b), which reports annual added capacity, shows that despite the decline in new plants, newly added capacity has risen over time, with some recent flattening (not for solar). Panel (c) shows that the average capacity per plant increased substantially in recent years (the average plant had a capacity of around 25 MW for most of our sample period, this number has increased to about 75 MW between 2020 and 2025). Hydro has the highest average capacity, followed by wind and then solar. Solar plants experienced the most pronounced growth in average capacity to more than 50 MW by 2025. Finally, Panel (d) illustrates the cumulative capacity growth.

[11] Utility-scale RE capacity excludes small installations serving individuals or businesses, such as most roof-top solar panels.

1.2 Remote Sensing Data

We use satellite imagery from two Earth observation programs to identify and quantify the Land Use and Land Cover (LULC) change caused by the construction of RE plants. First, the Sentinel-2 mission program of the European Space Agency provides multispectral imagery with a resolution of 10 to 60 meters. Its 13 spectral bands are well-suited to our study as they provide detailed LULC classification and its revisit frequency of 5 days with a two-satellite constellation ensures that land change detection is not disturbed by weather. Second, the Landsat program of NASA offers a continuous archive of Earth observation data since 1972, providing a long-term historical record for analyzing land change. Recent missions (Landsat 8/9) provide multispectral data primarily at 30-meter resolution with an 8-day combined revisit frequency. Both programs provide openly accessible data. Because Sentinel-2 offers finer spatial detail and more frequent revisits, we use its imagery for years from 2015 (unavailable in prior years). For satellite imagery before 2015, we use Landsat imagery.

2. Methodology

This section describes how we identify the biodiversity impact of RE power plants. We provide a relatively detailed explanation, as we introduce new data and methods to the finance literature. We explain how we (i) calculate the land use of RE plants and—as benchmarks—that of fossil-fuel-based and nuclear plants, (ii) determine the land type on which a facility was built, and (iii) translate the type-specific land use into biodiversity impact using a biodiversity metric.

2.1 Land-Use Calculations

2.1.1 Land Use of Solar Plants

Land use for solar farms with a capacity of at least 10 MW is calculated by combining latitude/longitude information from S&P MI with Sentinel-2 satellite imagery (as of 2024). The process involves several steps. First, we use the satellite imagery to search for solar panels within a 10 km buffer around each plant coordinate. Second, we employ a Random Forest machine learning algorithm on the Google Earth Engine (GEE) to classify pixels and identify solar

panels. The model utilizes Sentinel-2 spectral features and is trained and validated against the Global Photovoltaics Inventory (GPI) solar panel dataset (Kruitwagen et al., 2021). To enhance detection accuracy, particularly for installations constructed after 2018 (the end of the GPI's data coverage), we also incorporate Dynamic World LULC data (Brown et al., 2022).[12] Third, we manually verified the land use boundaries of all identified solar farms. For inaccurate detections, we adjust the solar panel boundaries to ensure we capture the actual footprint.[13]

For solar plants with a capacity below 10 MW, because their small size makes identification on satellite imagery prone to errors, we estimate land use with a log-linear regression model. This model uses a plant's capacity and its year of commercial operation start as explanatory variables. To calibrate the model, we use the directly measured land use of solar plants with a capacity above 10 MW together with their capacity and start year of operations. Details about this process are provided in Internet Appendix IA.C.

S&P MI also contains some commercial rooftop solar plants. As these plants sit on top of pre-existing built infrastructure, they do not displace natural habitat. Attributing biodiversity loss to such plants would therefore overstate the harm caused by the generating unit. We identify such plants, retain them in the sample so they contribute to capacity totals, but set their biodiversity impact to zero (see Internet Appendix IA.F.2 for details).

2.1.2 Land Use of Wind Plants

The land use of wind farms due to turbine foundations and access roads is typically highly dispersed, making direct detection and quantification from medium-resolution satellite data challenging.[14] Therefore, we apply an indirect estimation based on data from the National Renewable Energy Laboratory (NREL) of the U.S. Department of Energy (Denholm et al., 2009; Lopez et al., 2021). These data provide verified benchmark values for the land use of U.S. wind

[12] Dynamic World LULC data is used to compare land cover changes between the pre- and post-installation periods, which helps us to identify and manually correct inaccuracies in the initial detection.

[13] Figure IA.A.1 illustrates this process. If two plants are detected within 10 km of each other, we combine their areas and allocate the land use based on their respective capacities, we apply this approach as we are unable to distinguish the land use of plants located close to each other with satellite images (see Figure IA.A.2 for an illustration).

[14] By focusing on biodiversity effects of land use, we do not directly consider the effects from birds flying into the rotors of a wind plant. However, the biodiversity metric we employ indirectly captures the biodiversity value of the birds that live in the area of a wind plant.

farms. Since no comparable data are available globally, we assume that the land use of wind plants in and outside the U.S. is comparable. We consider the area of the turbine pads, service roads, and temporary installations that likely have a lasting impact on biodiversity. Using the NREL benchmark values, we calculate land use based on the number of wind turbines, which we determine by dividing the total plant capacity by the capacity of the specific turbine model that is used, and the land type on which they are constructed.[15] For units where turbine-specific data is unavailable, we estimate the land use based on their capacity, weighted land type, and the NREL benchmark values. Figure IA.A.3 illustrates the process.

2.1.3 Land Use of Hydropower Plants

For hydro plants, the primary land use arises from the inundation caused by the reservoirs, which we quantify by measuring the change in permanent water surface area from before to after dam construction using the JRC Yearly Water Classification History dataset (Pekel et al., 2016).[16] This dataset provides high-resolution (30 meters) maps of surface water locations since 1984. The process involves several steps. First, we calculate the inundated area as the increase in permanent water surface area between the pre- and the post-construction periods (using satellite imagery at the time of commercial operation compared to 10 years earlier). Second, we consider only the inundation of natural land cover types and not land types that were classified as built (urban/built-up) before the plant's construction (see Section 2.2). Third, if a dam serves multiple facilities, we allocate the total inundated natural land area among plant units based on their respective capacities (this ensures, for example, that we do not double count the biodiversity impact of a dam with two turbines). Figure IA.A.4 illustrates the process.

[15] Turbine model information in S&P MI is available for about 70% of the wind plant units. The capacity per turbine is obtained from the Wind Turbine Models database. The NREL benchmark values show that land use per turbine on bareland is 12,750 m^2, 22,050 m^2 for forest, 12,075 m^2 for grassland, and 14,400 m^2 for cropland (given an average capacity of 1.5 MW per turbine).

[16] As our methodological approach focuses on horizontal impacts on habitat loss through submerged areas, we do not quantify any potential habitat impact from the vertical dimension of a dam (dam heights and dam water levels can influence ecological effects beyond the inundated surface area).

2.1.4 Benchmarks: Land Use of Fossil-Fuel and Nuclear Plants

As benchmarks, we estimate the land use of fossil-fuel (gas, oil, coal) and nuclear plants. These facilities are predominantly thermal power plants with similar land use characteristics. Because smaller fossil-fuel-based plants are difficult to locate on satellite images, we only include those with a capacity of at least 100 MW in S&P MI. We then create a training dataset of 100 medium-sized plants (between 100 and 1,000 MW) and 100 large plants (more than 1,000 MW) and measure their land use by manually delineating their boundaries in satellite imagery. Figure IA.A.5 illustrates the delineated boundaries for four example plants. Second, we use information on the actual land use of the plants in the training dataset to calibrate a log-linear regression model in which a plant's capacity and year of construction serve as explanatory variables (separately for medium-sized and large plants). Third, we estimate the land use of 9,140 fossil-fuel and nuclear plants based on this calibrated model. Details are provided in Internet Appendix IA.D.

2.2 Land-Type Detection

To estimate biodiversity impacts, we need to determine the land *type* on which a facility was built. This information is important for differentiating between plants built on artificial land (like existing built-up areas with no or very little biodiversity value) and those constructed on natural/semi-natural habitats (like forest, grassland, or bare land). For years until 2020, we rely on the GLAD Global LULC dataset (Potapov et al., 2022), which is derived from the Landsat satellite data archive and quantifies changes in key land cover types with a 30-meter resolution. We reclassify their detailed land classes into seven categories: artificial (urban/built-up/reclaimed)[17], bare (bare ground), crops (cropland), grass (grassland/shrubland), trees (forest), snow/ice, and water. For years after 2020, we complement the GLAD dataset with data from the Dynamic World Project (Brown et al., 2022), which provides near-real-time global LULC classifications at 10-meter resolution using Sentinel-2 data.

Table IA.A.1 shows the distribution of the land types associated with RE plants. In Panel A, we show the overall land use in km^2 and Panel B the relative land use in %. The total land use

[17] Internet Appendix IA.F provides details on how we detect plants built on artificial land.

of all RE plants is about 27,137 km^2, equivalent to the area of Belgium. The most common land use of RE plants is grass land (27.5%), followed by crop land (21.4%), and forested land (18.9%). About one-tenth of the total area of RE plants is on artificial land. Since the biodiversity value of such artificial land is virtually zero, we consider this in the impact calculations. Snow, ice, and water play a minor role for RE plants.[18] When considering individual RE technologies, forested areas are the most common land types for hydro plants (42.2%), and grass land for wind (40.2%) and solar plants (29.1%).

2.3 Translating Land Use into Biodiversity Impacts

We quantify the biodiversity impacts due to land use by applying the STAR metric (Mair et al., 2021). Using a spatially explicit framework, this metric assesses the possible impact of threat reduction and habitat restoration activities on decreasing the extinction risk faced by species (as species, the framework considers mammals, amphibians, and birds). The STAR metric has been validated and applied in different conservation settings to evaluate biodiversity frameworks or extinction risks (e.g., Mair et al., 2023; Asefa et al., 2025). It is therefore emerging as a critical tool with high scientific grounding for investors and firms to evaluate their biodiversity impacts (Kashyap et al., 2025). It is presented, for example, as a tool for measuring biodiversity impact by the Taskforce on Nature-related Financial Disclosures (TNFD), which provides nature-related disclosure guidelines, or the Finance for Biodiversity Foundation (FfBF), an organization supported by financial institutions representing over $25 trillion in assets. Importantly, the STAR metric is available at a global level and scalable across time and geographies.[19]

The STAR metric consists of a Threat Abatement ($STAR_T$) and a Habitat Restoration ($STAR_R$) score, and we focus on $STAR_T$ because it better reflects biodiversity impacts of newly constructed infrastructure. STAR data is obtained via the Integrated Biodiversity Assessment Tool (IBAT).[20] A high $STAR_T$ score indicates locations that contain many threatened species,

[18] The reason why some area is on water is the same as for built land; we only exclude RE plants for which the coordinates are located on water, which does not exclude that part of a plant is constructed on water.

[19] In Internet Appendix IA.B, we discuss potential alternative biodiversity metrics and illustrate why the STAR metric is most appropriate in our context.

[20] Data on IUCN Red List of Threatened Species, Protected Area, and Key Biodiversity Area are also downloaded from IBAT, which are provided by BirdLife International, Conservation International, IUCN and UNEP-WCMC.

a high proportion of such threatened species' ranges, and a high severity of threats to those species (we verify this below). As a result, measures that prevent threats to biodiversity—in our case from new RE infrastructure—are especially effective in these regions. The STAR metric relies on the IUCN Red List of Threatened Species, which provides a globally recognized standard for assessing species' extinction risk. The scores are available at high "pixel" granularity and for a global raster with a base resolution of 5 km—each pixel therefore represents 5×5 km^2 on the ground. For each pixel, the proportion of a species' global area of habitat located in that specific pixel is then calculated and weighted by its IUCN Red List category score. The STAR$_T$ index value for each 5×5 km^2 pixel is in turn calculated as the sum of these species-specific scores (the foundational is therefore per-se a unit-less index).[21] Figure IA.A.6 illustrates the global STAR$_T$ score distribution, with blue color indicating low, and red color high, scores.

To calculate a STAR$_T$ score for a plant unit, we proceed in three steps. First, we overlay the calculated land-use footprint onto the global STAR$_T$ map layer at a resolution of 5 km^2. Second, we set STAR$_T$ scores to zero for any portion of the land use area that was classified artificial, because such land has typically little or no biodiversity value. Third, we calculate the total STAR$_T$ score for each plant unit as the aggregated STAR$_T$ score multiplied by the area of the land-use footprint (in m^2). A higher value indicates that preventing the construction of a plant would contribute more to the mitigation of global extinction risk; in other words, larger values can be interpreted as reflecting projects with potentially more negative biodiversity impacts. As additional measures, we calculate for each plant the STAR$_T$ density (STAR$_T$/1,000m^2), calculated as the total STAR$_T$ score divided by its footprint area (in 1,000 m^2). Additionally, we calculate the STAR$_T$ intensity (STAR$_T$/MWh) of a plant as the total STAR$_T$ score divided by its expected annual generation (in MWh).[22]

[21] Critically-endangered, endangered, vulnerable, or near-threatened species receive scores from 400 down to 100, respectively, while Least Concern species receive a score of zero. If a 5×5 km^2 pixel contains, for example, 0.5% of a critically-endangered species' global habitat ($0.005\times400=2$), 1% of a near-threatened species' habitat ($0.01\times100=1$), and 5% of a least-concern species' habitat ($0.05\times0=0$), the STAR$_T$ value for that pixel would be 3.0 ($=2+1+0$).

[22] The expected generation is based on a plant's capacity and technology-specific capacity factors (i.e., a plant's actual electricity output over a specific period divided by the maximum output if it would always run at full capacity). It is important to scale by expected generation, not actual capacity, since there is substantial heterogeneity in capacity factors across technologies. We rely on capacity factors from the EIA, which are 38% for hydro, 25% for solar, 34% for wind, 60% for fossil-fuel, and 92% for nuclear plants.

Given the somewhat abstract nature of the $STAR_T$ score, we show in Table IA.A.2 how it correlates with alternative species-based measures. In Columns (1) and (2), we use the number of species and threatened species affected by the siting of a RE plant, two simpler yet less precise measures of biodiversity impact.[23] The $STAR_T$ score is highly positively correlated with both measures, which corroborates that $STAR_T$ indeed captures impacts on species, especially threatened ones (species are classified as threatened based on IUCN classification). In Column (3), we use a threat-weighted species score, which combines species-habitat overlap with IUCN threat-status weights. We then sum these values across all affected species. Again, we find a high positive correlation. In Column (4), we show a high correlation with the $STAR_R$ score of the potential that habitat restoration in an area has on reducing global species extinction risks.

3. Evidence on Biodiversity Impacts of RE Plants

This section quantifies the biodiversity impact of existing and planned future RE plants and evaluates the impact by technology and over time.

3.1 Plant-Level Biodiversity Impacts

Using our new methodology, Table 1 reports plant-level statistics of the biodiversity impact of RE power plants. We calculate that the average RE plant has a $STAR_T$ score of about 105,040. However, the underlying distribution is highly skewed, with a 25^{th} percentile value of 70, a median of 1,100, and a 75^{th} percentile value of 10,640. Hence, the large average biodiversity impact of RE is driven by a few plants with very large $STAR_T$ scores.[24] $STAR_T$ scores per MWh of expected generation are also highly skewed, with a mean value of 13.73 and a median of 0.10, and the same holds for $STAR_T$ scores per 1,000 m^2 (mean of 442.32 and median of 7.44). Overall, the statistics indicate that the average plant is placed in an area with relatively low biodiversity value, while some plants are sited in locations with extremely high biodiversity

[23] We calculate the spatial intersection between each plant's land-use footprint and IUCN species habitat maps. We then quantify the number of affected species per plant.

[24] Because of this skewness, we use a log transformation in subsequent regressions. The log transformation is undefined for 3,175 observations for which the $STAR_T$ score equals zero, which can be the case when the whole RE plant is on artificial land or on land with a $STAR_T$ score of zero.

value. We explore this in more detail below.[25] Evidence on biodiversity impacts by technology and continent is reported in Table IA.A.4 and Table IA.A.5, respectively.

Table 2 lists the ten plant units with the largest land-use-induced biodiversity impacts. The plant with the largest overall impact is the Pachamama II Solar Project, a solar farm in Mexico, with a capacity of 330 MW and STAR_T score of 120.8 million. The hydro plant with the largest biodiversity impact is El Cajon in Mexico—in our sample as two units due to the two turbines employed—with a combined STAR_T score of about 119.9 million. Some top-ranked plants have a very large biodiversity impact despite small capacities. For example, the Mangilao Solar Plant in Guam has a capacity of only 60 MW but a STAR_T score of 116.3 million (see Figure IA.A.9).[26] Conversely, very large plants can have only limited biodiversity impacts. An example is the Jinchang Jinchuan Solar Plant in the Gobi desert (see Figure IA.A.10), with a capacity of 200 MW but a STAR_T score of only 32,059. Hence, a large physical footprint in an ecosystem with low species richness implies a small biodiversity impact.

Table IA.A.6 lists the ten "states" where RE plants have the highest biodiversity impact. States are based on Administrative Level 1 boundaries (i.e., the largest subnational division of a country, such as states in the U.S.). The most affected state is California (U.S.), with a cumulative STAR_T score of 268 million, followed by Mahārāshtra (India) and Central Province (Sri Lanka) with scores of 190 and 154 million, respectively. While the high impact in California is explained in part by the state's very high RE capacity (31 GW), the biodiversity impact in Central Province comes from a low RE capacity (below 400 MW); in this state, effects originate mostly from hydro plants sited in areas with high biodiversity values. Figure IA.A.7 illustrates the spatial link between RE plants and biodiversity impacts by showing an overlay between RE plant locations and the STAR_T map layer for Southeast Asia.

To complement the STAR-based calculations, we use spatial data associated with the IUCN Red List—so-called mapped areas of habitat (AOH)—to directly assess the overlap between

[25] Summary statistics on other variables are also in Table 1. The average plant uses 0.57 km^2 of land, has a capacity of 34 MW, and an expected annual generation of 98 GWh, all of which are highly skewed.

[26] The high impact of this plant is due to its location in a globally significant biodiversity hotspot. Guam hosts a large number of species for its size. These species are often endemic with very small habitats, so any land use has a major impact. The two small plants at the bottom of the top-10 are either in a volcanic-valley area where many species have narrow island- and valley-specific ranges (Gran Canaria, Spain) or an area known for extremely high biodiversity and endemism (Sindhudurg, India).

RE plant footprints and the habitats of individual species. Table IA.A.7 lists the species for which most of the habitat area is affected by RE. Panel A includes species that are classified as threatened (vulnerable, endangered, critically endangered), while Panel B only includes species that are critically endangered. An example of an affected species is the endangered Nelson's Antelope Squirrel, which only lives in the San Joaquin Valley in California—a total of 215 km^2 (or 1.3%) of its habitat overlaps with RE plants.[27]

3.2 Aggregate Biodiversity Impacts

Table 3 reports a quantification of the aggregate biodiversity impact of RE. The total $STAR_T$ score across all currently existing plants amounts to 5.0 billion, of which hydro contributes 2.68 billion, solar 1.96 billion, and wind 0.36 billion. The total score is roughly equivalent to the biodiversity value of the forested area in Austria, and exceeds the biodiversity value of the entire land in Germany, Norway, or Poland. Table IA.A.3 illustrates the geographical variation of the total biodiversity impacts for the 30 countries with the highest aggregate $STAR_T$ score. The highest total impact is in the U.S., followed by India and China. This ranking partly reflects the relatively high capacity that has been added in those countries over the past years. However, some other countries have high impacts despite low capacities (e.g., Sri Lanka or Costa Rica).

The quantified biodiversity impacts are sizable but might not appear dramatic in aggregate. However, this is likely to change given the projected expansion of RE. To gauge RE's potential future impact, we conduct an analysis based on the most recent data about planned and forecasted RE plants. We quantify different scenarios. In a first scenario, we add to existing RE plants those plants classified as "planned" in S&P MI as of Q1 2026. For these planned plants, we can use data on their intended locations. To estimate the land use of solar and hydro plants, we rely on an indirect method because they are not yet visible on satellite images (Internet Appendix IA.E provides details). This indirect method predicts the area of these planned plants based on their planned capacities. For planned wind plants, we use the method as for existing plants because this approach does not require satellite images. Table 3 shows that adding those

[27] Figure IA.A.8 visualizes the overlap between the area of habitat of the Nelson's Antelope Squirrel and RE plants in California.

planned plants will increase the total biodiversity impact of RE from 5.0 billion to 7.4 billion, with the new total being equivalent to the biodiversity value of the entire land area in Senegal.

In the second scenario, as an alternative to adding planned plants from S&P MI, we use near-term predictions from the IEA. This approach is complementary as S&P MI might not include all planned plants. According to the main case of IEA's Renewable Energy Progress Tracker, about 130 GW of hydro, 600 GW of onshore wind, and 1.7 TW of utility-scale solar capacity will be added from 2026 until 2030. Since we neither have coordinates nor country information for where this capacity is expected to be sited, we multiply the predicted new capacity with the average STAR_T value per capacity for each technology. Adding the resulting impacts to the current figures increases the total STAR_T score of RE from currently 5.0 to 14 billion by 2030.

In the third scenario, we rely on the IEA's World Energy Outlook 2025 long-term projection for RE generation in 2050. Based on predicted wind and solar generation, we calculate future capacities and then multiply those with the average STAR_T value per capacity for each technology. Since there is no prediction for hydro, we assume that this technology's growth rate from 2025 to 2030 continues until 2050. For this scenario, we calculate that the total STAR_T score of RE exceeds 50 billion by 2050, equivalent to the biodiversity value of the entire land area in Canada or Uganda.

3.3 Biodiversity Impacts by Technology

Differences in biodiversity impacts across solar, wind, and hydro are important to understand, because each technology affects ecosystems in unique ways due to differences in land use and plant locations. Understanding these differences allows RE planners, investors, and policymakers to select appropriate sites, design effective mitigation measures, and balance RE development with ecosystem protection. Documenting and recognizing these variations is essential to ensure that RE contributes to both climate change mitigation and biodiversity conservation.

We quantify technology-specific impacts in Figure 3. In Panel (a), which includes fossil-fuel and nuclear power plants as benchmarks, we aggregate the STAR_T scores across plants and allocate them to different technologies. Hydro plants account for 52.9% of the total impact, followed by solar with 38.7%. Wind plays a negligible role (7.2%) as do non-RE plants (1.2%),

primarily due to limited land use.[28] Panel (b) plots by technology the mean, 25^{th} percentile, median, and 75^{th} percentile of the STAR_T score per plant. In line with Panel (a), the average impact per plant is highest for hydro, followed by solar and wind. Notably, the impacts of all technologies are highly skewed. For the STAR_T score scaled by expected generation in Panel (c), hydro continues to have the highest average biodiversity impact, followed closely by solar. Wind and non-RE plants have much lower STAR_T values per unit of generation. For land use per plant in Panel (d), solar plants require most space, followed by hydro and wind. Panel (e), which considers impact per 1,000 m^2 of land use, shows that hydro plants are located in the most biodiversity-sensitive areas: the median STAR_T value per 1,000 m^2 is 72 for hydro plants, but five or less for solar, non-RE, and wind. A conclusion is that the biodiversity impacts are largest for hydro and solar. Whereas the impact of hydro comes mostly from siting in biodiversity-sensitive areas, the impact of solar is driven by high land use.

Table 4, Panel A, complements the figures with regressions using indicators for solar, wind, or hydro plants (fossil-fuel-based and nuclear plants are the omitted benchmark). In Column (1), we explain the STAR_T score of a plant using these indicators. In Column (2), we add fixed effects to compare plants in the same country and year, to ensure the estimates are unaffected by endogenous technology choices (e.g., countries with high solar irradiation might have higher biodiversity values and solar plants are more likely to be sited where solar irradiation is high). In Column (2), the coefficients imply that the STAR_T value of solar plants is more than ten times that of non-RE plants, and for hydro plants it is about six times. For wind plants, the STAR_T values are only about three times higher. In Column (3), when controlling for a plant's expected generation, the differences increase further, with solar (hydro) plants having STAR_T values that are several hundred times (ninety times) higher than those of non-RE plants. The increase in effect size arises because RE plants generate substantially less electricity per unit of land use than non-RE plants. When we alternatively use STAR_T scores scaled by expected generation (in MWh) in Column (4), results are in line with those in Column (3). In Column (5), we explain the STAR_T score scaled by land use, to measure how biodiversity-sensitive

[28] It is important to emphasize that fossil-fuel-based power plants affect biodiversity primarily through the emissions they generate, which constitutes an impact dimension not reflected in this comparison.

the area of a plant is (ignoring the size of the plant). We find that hydro plants are sited in more biodiversity-sensitive areas compared to non-RE plants, while wind and solar plants typically locate in areas with similar biodiversity values as non-RE plants. Overall, the regressions confirm that hydro plants are sited in the most biodiversity-sensitive areas, but solar plants are on average most detrimental to biodiversity due to their high land use.

3.4 Biodiversity Impacts over Time

It is important to understand how the biodiversity impacts of RE plants evolved over time, to gain insights into whether changes in technology, policy, or environmental awareness have improved the impact of RE. For example, it might be that early RE projects paid little attention to ecological consequences, while over time, as knowledge or monitoring increased, developers adjusted siting practices to factor in the biodiversity value of an area.

Figure 4 shows different measures of the time-series of biodiversity impacts of RE plants. Panel (a) plots the total STAR_T score of all plants that started operation in a given year. The total impact of all RE plants increased three-fold over time. Hydro accounted for the vast majority of the impact in the first half of the sample period and solar overtook hydro in terms of impact in the late-2010s. Wind played a minor role in all years. Panel (b) shows cumulative STAR_T scores over time, highlighting that while the negative biodiversity impact of hydro plants is leveling off since the 2010s, solar's impact is accelerating rapidly. Panel (c) shows that also the mean STAR_T score across all RE plants increased over time. For solar plants, the increase is most pronounced. In Panel (d), which scales the STAR_T score by expected generation (in MWh), we find an increasing trend for solar plants and a decreasing trend for hydro plants (with an outlier in 2023). Across all RE plants, the STAR_T per MWh is relatively constant over time, which indicates that the increase in the average biodiversity impact comes mostly from increasing capacity. This is in line with the increasing land use of RE plants displayed in Panel (e): on average, RE plants grew from less than 0.5 km^2 per plant in 2000 to approximately 2 km^2 in 2025 (from 0.2 km^2 to 2.5 km^2 for solar plants). In terms of the STAR_T score per 1,000 m^2, Panel (f) shows that there is a slight decreasing time trend. These findings indicate that the upward trend in overall biodiversity impact of RE plants over time comes mostly from

increasing land use, not from siting in more biodiversity-sensitive locations.

Table 4, Panel B, complements the figures with regressions. In Column (1) and (2), the STAR_T score increased substantially over time, by about 10 % per year without fixed effects and 4% with fixed effects. When we control for capacity in Column (3), the time trend becomes statistically insignificant, which indicates that the increase in Columns (1) and (2) is driven by higher capacities. For STAR_T score scaled by expected generation in Column (4), we find a small decreasing trend of about 2% per year. In Column (5), we observe that siting decisions became less biodiversity-friendly over time when comparing plants in the same countries using the same technologies (which explains why this trend was not visible in the previous graphical analysis). However, the statistical significance and economic magnitude are small. Overall, in line with Figure 4, the increasing biodiversity impact of RE plants is mainly driven by higher land use due to higher capacity, though there is also some evidence of plants being constructed in more biodiversity-sensitive locations over time.

One potential reason why new RE plants have been sited in more biodiversity-sensitive areas within countries could be a lack of alternative options, especially where RE expands rapidly. Table 4, Panel C, considers this explanation by controlling for the share of RE capacity in a country's total capacity three years before the start of a plant's operation. In Column (1), we indeed find a higher biodiversity impact of new plants in countries where the existing RE share is higher: a one-percentage-point increase in the RE capacity share is associated with locations of new plants that have a 1% higher STAR_T score. This conclusion is unchanged with country, year, and technology fixed effects in Column (2), when controlling for a plant's expected generation in Column (3), using the logarithm of the STAR_T score per MWh of expected generation in Column (4), or using the STAR_T score per 1,000m^2.

4. Evidence on Impact Concentration and Counterfactual Analysis

This section documents that the biodiversity impact of RE is highly concentrated among a few plants. It then provides a counterfactual analysis to estimate the potential mitigation achievable if the highest-impact solar and wind plants had been sited in nearby areas.

4.1 Plant-Level Concentration of Biodiversity Impacts

Table 1 highlights skewness in the biodiversity impact of RE plants. We now build on this observation and explore economic drivers of this heterogeneity. Table 5, Panel A, reports coefficients of variation (CV)—the standard deviation divided by the mean—across RE plant units for the STAR_T score, the STAR_T score scaled by expected generation, and the STAR_T score scaled by land use. The CVs confirm highly skewed distributions. Across all RE plants, the standard deviation of absolute STAR_T scores is more than 12 times larger than the mean. Similarly, the CVs for STAR_T scaled by generation and land use are 17 and 8, respectively, confirming substantial overall dispersion in the data.

To understand the drivers of this heterogeneity, we analyze within-group variation by restricting the sample to plant units sharing the same technology, commercial operation start year, or geographic location (country, state, or region). Within-technology and within-year variation remain comparable to the overall variation, that is, the overall variation is not driven by differences in technology or by time trends in biodiversity impacts. However, introducing geographic restrictions reduces the dispersion: the CV declines slightly when limiting the sample to the same country, and drops more noticeably at the state and regional levels; this suggests that large parts of the impact variation are driven by spatial differences in biodiversity. Finally, we evaluate highly restrictive, multidimensional groupings. Among plants sharing the same technology, start year, and country, the CV across all measures falls to about three. Replacing the country-level restriction with finer state- and region-level boundaries further reduces the CV to about one or slightly below one, respectively. Nevertheless, even under these most stringent specifications, substantial variation in biodiversity impacts persists across individual plants, making it important to understand the drivers of this residual variation.

One driver of the residual variation could be a small number of plants with very high impacts. We therefore next quantify the concentration of biodiversity impacts across individual plants. Impact concentration is important economically and environmentally, because it can determine where and how developers, investors, or policy makers can respond to any biodiversity effects. If most of the impact is caused by a few plants, then targeted mitigation measures—such as

adjusting siting or restoring local habitats—can address the issue. It would also allow restoration resources to be focused where they will have the greatest effect. However, if the impacts are widespread across many plants, it suggests a systemic problem that requires broader policy or planning changes (e.g., new siting standards or improved environmental assessments).

To address this question, we report in Table 5, Panel B, the share of the overall STAR_T score attributable to the top-10, top-100, and top-500 plants with the highest score; we also report how much of the overall RE capacity these plants account. The numbers we obtain are striking. The ten plants with the highest STAR_T score account for 13.2% of the total STAR_T score, but only provide 0.2% of total capacity. The corresponding numbers for the top-100 (top-500) plants are 40.9% (68.6%) for the STAR_T score share and 0.8% (3.1%) for the capacity share. When we consider the top-1% of plants, they account for 67.9% of the total STAR_T score but only 2.9% of the total capacity. This shows that a very limited number of plants account for the vast majority of the biodiversity impact of RE.[29] This implies that RE's biodiversity impact could have been substantially reduced if the worst projects had been sited elsewhere. It also suggests that restoration resources should be focused to have the greatest overall effect.

4.2 Counterfactual Siting for Wind and Solar Plants

Given the extreme impact concentration, we conduct a counterfactual analysis to estimate the potential mitigation achievable if the highest-impact solar and wind plants had been sited in nearby areas with lower biodiversity values. We exclude hydro plants from this exercise due to their strict topographical and hydrological constraints, which generally prohibit construction in alternative locations. Because not all land is suitable for wind and solar development, our counterfactual search is limited to locations where construction is technically feasible. Internet Appendix IA.G provides details on how we identify such locations.

Focusing in Table 6, Panel A, on a 10 km radius for counterfactual locations, we calculate the percentage difference between a plant's actual STAR_T score and that of an equally sized counterfactual site. The counterfactual site is defined as the location within the 10 km radius

[29] In line with our other analyses, we conduct this test on the power plant *unit* level. An analysis at the plant level reveals an even higher concentration. For instance, 72.5% of the biodiversity impact comes from the top-1% of plants.

that minimizes the STAR_T score. We find that an alternative siting of the top-1% most damaging plants to their respective optimal counterfactual sites would result in an 86.2% reduction in their STAR_T scores. This translates to a 55.1% reduction in the total biodiversity footprint of all wind and solar plants. Even when incorporating hydro into the baseline, relocating just this worst 1% of wind and solar plants reduces the total RE impact by 25.6%. Expanding the counterfactual analysis to the worst 5% and 10% of plants yields slightly smaller reductions at the plant level—further confirming the extreme concentration of impacts at the very tail of the distribution. However, the aggregate reductions in the total wind and solar footprint increase to 69.5% and 73.9%, respectively (32.3% and 34.3% reductions in the total RE footprint). In Panels B and C, we expand the search radius to 20 km and 50 km, which naturally yields even larger mitigation potentials. Figure 5 illustrates the counterfactual analysis for a 10 km radius using the Ichigo Nago Futami solar plant in Japan. Choosing the counterfactual site reduces its STAR_T-based impact from 19.1 million to 0.3 million, a 98% reduction.

Our results underscore the large mitigation potential from simply avoiding a small number of high-impact sites. While relocating existing infrastructure is technically complex and economically prohibitive, the counterfactual exercise illustrates the critical importance of ex-ante biodiversity screening. As we show, when projects are proposed in ecologically sensitive regions, lower-impact alternative sites are often available within a short distance. Therefore, mitigating the ecological footprint of RE does not require halting the energy transition or compromising energy security and climate targets. Rather, our results advocate for the careful exploration of nearby, lower-impact alternatives prior to finalizing construction in biodiversity-sensitive areas. This is an area where attention from investors and regulators can yield substantial environmental benefits.

5. Evidence on Impact Heterogeneity across Firms

This section examines *firm-level* variation and concentration of biodiversity impacts, and the role of cross-sectional heterogeneity in ownership structures and the financing of RE plants. This analysis serves a dual purpose. First, it sheds light on whether biodiversity risk is an unavoidable

by-product of RE investments or instead a firm-specific risk that can be mitigated via screening and selection of low-impact firms. Second, it provides insights into the role of three dimensions of heterogeneity: the source of equity capital (listed versus unlisted), ownership type (financial versus non-financial), and financing structure (project versus corporate finance). Our estimates are not causally identified, but we use high-dimensional fixed effects to mitigate potential biases.

5.1 Firm-Level Variation and Concentration of Biodiversity Impact

To understand the importance of screening and selection, we start with an analysis of cross-firm variation in biodiversity impacts. Table 7, Panel A, reports for STAR_T, STAR_T scaled by generation, and STAR_T scaled by land use the coefficient of variation (CV) across the firms owning RE plant units. As firms we consider the direct owners, who constitute the entities at the lowest-level in the ownership chain of a plant unit. We observe substantial heterogeneity based on the CV for the STAR_T score, with an extreme value of 9.48. Considering only firms' plants with the same technology or start year to calculate the CV does little to diminish the dispersion. When calculating cross-firm variation within the same geographic area, the CV declines substantially but remains above one, still indicating high variation. Simultaneously conditioning on technology, operational year, and geographic location further reduces dispersion but the residual variation remains above 0.6. Similar patterns hold for the other two measures. Overall, this demonstrates significant cross-sectional variation in firm-level biodiversity impacts, which are not fully explained by technology choices or geographic location. Consequently, careful screening of firms owning RE plants can mitigate biodiversity risks within an investment portfolio. As the firm-level biodiversity impact varies even within narrow regions, some investors might end up investing in "bad" high-impact firms, while others select "good" low-impact firms nearby.

A similar conclusion emerges from Table 7, Panel B, which reports the concentration of the biodiversity impact among RE firms (again defined as the direct owners). The top-10 firms with the highest STAR_T score account for 18.1% of the aggregate biodiversity impact, but only 0.9% of the total capacity. The corresponding numbers for the top-100 (top-500) firms are 58.6% (85.0%) for the STAR_T score share and 10.9% (37.2%) for the capacity share. When we focus on the top-1% (top-5%, top-10%) of firms with the highest impact, a similar pattern emerges. This

implies that the biodiversity impact of RE is concentrated among a limited number of firms. Motivated by this finding, we next examine ownership heterogeneity at more granular levels.

5.2 Unlisted versus Listed Firms

The first heterogeneity relates to RE plant ownership by listed versus unlisted entities. How listing status relates to biodiversity impacts is unclear ex ante. On the one hand, plants of listed firms may have a larger biodiversity impact. Shive and Forster (2020) document that listed firms are more likely to pollute, or to incur penalties from violating environmental regulations, compared to unlisted firms. They attribute this effect to governance and incentive differences: unlisted firms often have more direct accountability, which makes their owners more sensitive to reputational concerns and long-term considerations. Furthermore, listed firms might face stronger short-term pressures that can encourage cost considerations at the expense of environmental outcomes. On the other hand, plants of listed firms might have a lower biodiversity impact. Listed firms usually have more dispersed shareholders and these dispersed owners—as modeled by Kwok, Spiro, and van Benthem (2026)—might be more likely to take environmental factors into consideration for investment decisions (they suffer less profit loss compared to large owners for the same environmental benefit). Additionally, oversight by investors and regulators is likely more pronounced for listed firms, which could make them more hesitant to be exposed to biodiversity risks. For instance, Duchin, Gao, and Xu (2025) show that polluting assets are disproportionally often purchased by private buyers because they face less public pressure.

To classify firms into unlisted or listed, we rely on S&P MI, which contains the names of direct and ultimate owners of RE plant units as well as their equity stakes. We measure ownership three years before the start of commercial operation, because this typically corresponds to the moment when siting decisions are made. Our variable of interest, $\text{Listing}_{Direct/Ultimate}$, equals one if the firm that directly or ultimately owns a plant unit is listed at a public exchange, and zero otherwise.[30] If a plant unit has multiple firms as owners, we assign the biodiversity impact

[30] We additionally rely on an external ticker file (Compustat Global Link table) and manual research to deal with incomplete listing information. A challenge is that a firm's listing status can change over time; we classify this status based on the most recent information. In cases where a subsidiary is listed but its parent company is not (or vice-versa), only the directly listed entity is classified as public.

and production capacity to each firm according to ownership shares. We therefore consider in what follows each plant-unit-owner combination as one observation.

Table 8, Panel A, examines the link between listing status and biodiversity impact. In the regressions, we include region-by-technology as well as year-by-technology fixed effects. This ensures that we compare plant units of listed and unlisted firms within the same technology and region at a point in time. This is important as not all technologies are suitable for all locations (e.g., hydro requires very specific geological conditions) and some locations have higher biodiversity values than others (e.g., a concentration of listed firms in high-biodiversity areas creates a correlation between listing status and biodiversity impacts). In Column (1), which explains the STAR_T value, the biodiversity impact of plants owned by listed firms is nearly twice as high as that of those belonging to unlisted firms. However, controlling for electricity generation in Column (2) makes this difference disappear. STAR_T values scaled by generation or land use in Columns (3) and (4) also reveal no differences between plants of listed and unlisted firms. Collectively, these findings indicate that the higher absolute biodiversity impact of listed firms' plants is driven by scale: listed firms operate larger plants, which naturally have a larger environmental footprint, but they are not more damaging per unit of energy or land than unlisted firms.

Table 8, Panel B, exploits within-firm variation by comparing plant units owned by listed versus unlisted subsidiaries of the same ultimate parent firm.[31] Empirically, we achieve this by adding parent-by-year fixed effects. The results from this analysis are starkly different: across all biodiversity metrics, plant units owned by listed subsidiaries exhibit significantly lower impacts than those held by unlisted subsidiaries within the same corporate group. This suggests that ultimate parent firms strategically allocate their high-impact plants to private subsidiaries. Such behavior is consistent with attempts to shield environmentally damaging assets from the heightened investor and regulatory scrutiny present in public markets.

[31] NextEra Energy, for example, operates as an ultimate owner RE assets through a mix of listed (e.g., via XPLR Infrastructure) and unlisted (e.g., via Florida Power & Light Company) entities.

5.3 Financial versus Non-Financial Firms

The second analysis of ownership heterogeneity contrasts financial and non-financial firms.[32] This separation is motivated by prior literature emphasizing that financial firms face relatively higher environmental pressures. Specifically, prior work shows that the actions of financial firms are shaped by a complex mix of financial, reputational, and normative pressures. While their actions can be driven by financial motives (e.g., to reduce portfolio-wide climate risks), financial firms are also uniquely subject to non-financial pressures. These pressures can stem from their clients' social preferences, their own ethical considerations, and a strong desire to protect their reputations (Chen, Dong, and Lin, 2020; Krueger, Sautner, and Starks, 2020). Furthermore, their sensitivity to environmental issues is driven by social norms in their home countries, which they then transplant globally to their portfolio firms (Dyck et al., 2019). These distinct pressures should make financial firms more attentive to biodiversity considerations for their investments.

We rely again on ownership information from S&P MI to classify ownership types. Our variable of interest, Financial Owner$_{Direct/Ultimate}$, equals one if the direct or ultimate owner of a plant unit is a financial institution (bank, endowment fund, hedge fund, insurance company, mutual fund, PE fund, or pension fund), and zero otherwise. As before, to account for multiple owners in the same unit, we consider each plant-unit-owner combination as one observation.[33]

Table 9, Panel A, presents results. We find that plant units held by financial firms exhibit significantly lower biodiversity impacts compared to those held by non-financial firms. In Column (1), after controlling for expected generation, units owned by financial firms have a biodiversity impact that is about 10% lower. Panel B again compares plant units held by financial and non-financial entities of the same ultimate parent.[34] This specification yields similar, and economically even stronger, results. We now also find that plant units of financial firms locate in less biodiversity-sensitive areas. Hence, parent firms seem to house high-impact plant units in non-financial subsidiaries, possibly because they face less investor or regulatory scrutiny.

[32] Andonov and Rauh (2025) document that financial institutions such as private equity (PE) firms are important investors in RE in the U.S.

[33] In our sample, for 14.4% of plant-unit-owner links, there is a financial owner.

[34] An example of a corporate structure where a ultimate owner has equity stakes in a financial and a non-financial entity is Brookfield Corporation. The firm has a stake in TerraForm Power, a RE owner and developer (non-financial firm), and also in Brookfield Property REIT, an investment manager (financial firm).

5.4 Project Finance versus Corporate Finance

The final heterogeneity we explore relates to whether RE plants are project financed (off-balance sheet) or corporate financed (on-balance sheet). Project-financed plants are constructed in a separate company, typically a Special Purpose Vehicle (SPV). For plants financed through corporate finance, the investment is financed from the balance sheet of a parent company, without ring-fencing and separation through the SPV. How this financing dimension relates to biodiversity impacts is conceptually unclear. On the one hand, the investment horizon of SPV investors is usually relatively long, as the repayment and dividend distribution only comes from the project cash flows over time (Esty, 2004). Because of this longer horizon, investors in SPVs may face less short-term performance pressure, allowing them to more carefully evaluate biodiversity risks when making siting decisions. On the other hand, SPV structures can be used to move severe risks away from the sponsoring firm, as a large literature in banking shows. Furthermore, SPVs are structurally opaque, which shields them from the investor, regulatory, and public scrutiny that traditional firms typically face. From this perspective, SPV-backed projects might place less emphasis on mitigating biodiversity impacts and RE plants financed through them might exhibit worse biodiversity footprints. To distinguish project-financed from corporate-financed plant units, we rely on the classification by Heiss and Schmid (2025).[35]

Table 10 reports the relationship between a plant unit's financing structure and its biodiversity impact. Across all models, project-financed plants exhibit higher biodiversity impacts (e.g., an about 20% higher overall impact). When we exploit within-parent variation to compare project- and corporate-financed plants belonging to the same ultimate parent, we find similar results. Thus, when an ultimate parent firm invests in a high-impact RE plant, it is significantly more likely to structure the investment via an SPV. These findings are consistent with firms utilizing opaque, limited-recourse vehicles to place environmental risks.

[35] They use data from S&P MI and LSEG Infra 360. Because the latter database has limited coverage of smaller facilities, this classification is restricted to plant units with a capacity of at least 10 MW (about half of our sample). Within this sample, 29.2% of RE plant units are project-financed, while 70.8% are corporate-financed.

6. Conclusion

The transition to RE is the central pillar of climate change mitigation. However, pursuing these investments may involve environmental costs because RE plants can negatively affect biodiversity. These links indicate that mitigating climate change and biodiversity loss are closely intertwined. At this stage, however, large-scale, comprehensive evidence on the biodiversity impact of RE is lacking. We make progress towards closing this gap by constructing a novel global measure of the land-use-induced biodiversity impact of RE power plants, combining granular power plant location, remote sensing, and biodiversity data.

Our quantification shows that the RE plants generate a biodiversity impact, quantified as the aggregate STAR_T score across all plants, equivalent to the value of the forested area in Austria. We estimate that the projected impacts of RE could reach the scale of the biodiversity value of Canada's entire land area. Our approach is therefore not only relevant in quantifying the biodiversity impact of existing RE projects, but can also be used when evaluating future projects. We show that solar plants cause the greatest negative impact overall, while hydro plants are located in the most biodiversity-sensitive areas. The biodiversity impact of RE has grown substantially over time, driven by increased land use and siting in more biodiversity-sensitive locations. This impact is highly concentrated, with the top 1% of plants and firms responsible for the majority of the biodiversity effects. We further document systematic differences in how plants' ownership and financing choices affect their biodiversity impacts.

Appendix

Appendix A: Definitions of Variables

Variable	Description
STAR_T	STAR_T score of a power plant unit. STAR_T is the Threat abatement subscore of the STAR metric, which quantifies the potential contribution of threat mitigation actions toward reducing global species extinction risk (Mair et al., 2021). Source: Own calculations, IBAT.
$\frac{\text{STAR}_T}{\text{MWh}}$	STAR_T score of a power plant unit scaled by its expected electricity generation (in MWh). Source: Own calculations, IBAT, S&P MI, IEA.
$\frac{\text{STAR}_T}{1{,}000\text{m}^2}$	STAR_T score of a power plant unit scaled by its land-use area (in $1{,}000^2$. Source: Own calculations, IBAT, S&P MI.
STAR_R	Habitat restoration subscore of the STAR metric, which quantifies the potential contribution of habitat restoration toward reducing global species extinction risk (Mair et al., 2021). Source: Own calculations, IBAT.
# Species (All)	Number of species whose habitat overlaps with a plant unit's spatial footprint, regardless of IUCN Red List status. Source. Own calculation, IUCN.
# Species (TR)	Number of threatened species whose habitat overlaps with a plant unit's spatial footprint. Threatened species are defined as those classified as vulnerable (VU), endangered (EN), or critically endangered (CR) on the IUCN Red List. Source. Own calculation, IUCN.
Species Threat Score	Threat-weighted species-overlap score based on the spatial intersection between a plant unit's land-use footprint and species habitat maps. Source: Own calculation, IUCN, IBAT.
Land Use	Land-use area of a power plant unit in square meters. Source: Own calculation.
Solar/Hydro/Wind	Dummy variable that equals one if a power plant unit uses solar/hydro/wind as generation technology, and zero otherwise. Source: S&P MI.
Capacity	Capacity of a power plant unit in MW. Source: S&P MI.
Generation	Expected annual electricity generation of a power plant unit in GWh based on its capacity and technology-specific capacity factor. Source: Own calculation, S&P MI, EIA.
Share $\text{RE}^{t-3}_{Country}$	Renewable power plant capacity relative to the total electricity-generating capacity in the country in which the power plant unit is located. The variable is measured three years before a plant unit's start of commercial operation (approximately when the siting and other construction-related decision were made). Source: Own calculation, S&P MI.
$\text{Listing}_{Direct/Ultimate}$	Dummy variable that equals one if either the direct owner or ultimate parent company of the power plant unit is listed at a public exchange, and zero otherwise. Source: Own classification, S&P MI.
Listing_{Direct}	Dummy variable that equals one if the direct owner of the power plant unit is listed at a public exchange, and zero otherwise. Source: Own classification, S&P MI.
Financial $\text{Owner}_{Direct/Ultimate}$	Dummy variable that equals one if either the direct owner or ultimate parent company of a power plant unit is classified as a bank, endowment fund, hedge fund, insurance company, mutual fund, PE fund, or pension fund, and zero otherwise. Source: Own classification,Source: Own classification, S&P MI.
$\text{Financial Owner}_{Direct}$	Dummy variable that equals one if either the direct owner of a power plant unit is classified as a bank, endowment fund, hedge fund, insurance company, mutual fund, PE fund, or pension fund, and zero otherwise. Source: Own classification, S&P MI.
Project Financed	Dummy variable that equals one if a power plant unit is project financed (off-balance sheet), and zero if it is corporate financed (on-balance sheet). Source: Classification from Heiss and Schmid (2025).
Year COD	Year in which a power plant united started commercial operation. Source: S&P MI.

S&P MI stands for S&P Market Intelligence, EIA for Energy Information Administration, IUCN for International Union for Conservation of Nature, IBAT for Integrated Biodiversity Assessment Tool.

References

Andonov, Aleksandar, and Joshua D. Rauh, 2025, The shifting finance of electricity generation, NBER Working Paper.

Asefa, Addisu, Yilma Dellelegn Abebe, Abdeta Debella Robi, Melesse Maryo, Gemedo Dalle, Kumara Wakjira, Antonin Vergez, Florence Curet, and Mekbeb Tessema, 2025, Validating application of the species threat abatement and restoration (STAR) metric in meeting national biodiversity conservation targets, *Biodiversity and Conservation* 34, 2715–2738.

Berg, Tobias, Robin Döttling, Xander Hut, and Wolf Wagner, 2025, Do voluntary initiatives make loans greener? Evidence from project finance, Working Paper.

Brown, Christopher F., Steven P. Brumby, Brookie Guzder-Williams, Tanya Birch, Samantha Brooks Hyde, Joseph Mazzariello, Wanda Czerwinski, Valerie J Pasquarella, Robert Haertel, Simon Ilyushchenko, et al., 2022, Dynamic world, near real-time global 10 m land use land cover mapping, *Scientific Data* 9, 251.

Chaudhary, Abhishek, Francesca Verones, Laura De Baan, and Stefanie Hellweg, 2015, Quantifying land use impacts on biodiversity: combining species–area models and vulnerability indicators, *Environmental Science & Technology* 49, 9987–9995.

Chen, Fukang, Minhao Chen, Lin William Cong, Haoyu Gao, and Jacopo Ponticelli, 2025, Pricing the priceless: The financing cost of biodiversity conservation, Working Paper.

Chen, Tao, Hui Dong, and Chen Lin, 2020, Institutional shareholders and corporate social responsibility, *Journal of Financial Economics* 135, 483–504.

Cryan, Paul M., P. Marcos Gorresen, Cris D. Hein, Michael R. Schirmacher, Robert H. Diehl, Manuela M. Huso, David T.S. Hayman, Paul D. Fricker, Frank J. Bonaccorso, Douglas H. Johnson, et al., 2014, Behavior of bats at wind turbines, *Proceedings of the National Academy of Sciences* 111, 15126–15131.

De Palma, Adriana, Andrew Hoskins, Ricardo E Gonzalez, Luca Börger, Tim Newbold, Katia Sanchez-Ortiz, Simon Ferrier, and Andy Purvis, 2021, Annual changes in the biodiversity intactness index in tropical and subtropical forest biomes, 2001–2012, *Scientific Reports* 11, 20249.

Denholm, P., M. Hand, M. Jackson, and S. Ong, 2009, Land use requirements of modern wind power plants in the United States, National Renewable Energy Lab.

Díaz, Sandra, Josef Settele, Eduardo S Brondízio, Hien T Ngo, John Agard, Almut Arneth, Patricia Balvanera, Kate A Brauman, Stuart HM Butchart, Kai MA Chan, et al., 2019, Pervasive human-driven decline of life on earth points to the need for transformative change, *Science* 366.

Duchin, Ran, Janet Gao, and Qiping Xu, 2025, Sustainability or greenwashing: Evidence from the asset market for industrial pollution, *Journal of Finance* 80, 699–754.

Durán, América P, Jonathan MH Green, Christopher D West, Piero Visconti, Neil D Burgess, Malika Virah-Sawmy, and Andrew Balmford, 2020, A practical approach to measuring the biodiversity impacts of land conversion, *Methods in Ecology and Evolution* 11, 910–921.

Dyck, Alexander, Karl V. Lins, Lukas Roth, and Hannes F. Wagner, 2019, Do institutional investors drive corporate social responsibility? International evidence, *Journal of Financial Economics* 131, 693–714.

Esty, Benjamin C., 2004, Why study large projects? An introduction to research on project finance, *European Financial Management* 10, 213–224.

Flammer, Caroline, Thomas Giroux, and Geoffrey M. Heal, 2025, Biodiversity finance, *Journal of Financial Economics* 164, 103987.

Frank, Eyal, and Anant Sudarshan, 2024, The social costs of keystone species collapse: Evidence from the decline of vultures in India, *American Economic Review* 114, 3007–3040.

Garel, Alexandre, Arthur Romec, Zacharias Sautner, and Alexander F. Wagner, 2024, Do investors care about biodiversity?, *Review of Finance* 28, 1151–1186.

Garrett, Daniel, and Sophie Shive, 2026, Clean energy development and biodiversity: Economic tradeoffs, Registered Report Draft.

Gasparatos, Alexandros, Christopher NH Doll, Miguel Esteban, Abubakari Ahmed, and Tabitha A Olang, 2017, Renewable energy and biodiversity: Implications for transitioning to a green economy, *Renewable and Sustainable Energy Reviews* 70, 161–184.

Giglio, Stefano, Theresa Kuchler, Johannes Stroebel, and Oliver Wang, 2026a, Nature and biodiversity loss: A research agenda for financial economics, *Journal of Finance: Insights and Perspectives,* forthcoming.

Giglio, Stefano, Theresa Kuchler, Johannes Stroebel, and Xuran Zeng, 2026b, Biodiversity risk, *Review of Finance* 30, 131–161.

Heiss, Alexander, and Thomas Schmid, 2025, Project finance revisited, Working Paper.

Hernandez, Rebecca R., Madison K. Hoffacker, Michelle L. Murphy-Mariscal, Grace C. Wu, and Michael F. Allen, 2015, Solar energy development impacts on land cover change and protected areas, *Proceedings of the National Academy of Sciences* 112, 13579–13584.

IEA, 2024, Renewables 2024: Analysis and forecasts to 2030, Technical report, International Energy Agency.

IEA, 2025, World Energy Outlook 2025, Technical report, International Energy Agency.

IEA, 2026, Renewable energy progress tracker, Technical report, International Energy Agency.

IRENA, 2025, Delivering on the UAE consensus: Tracking progress toward tripling renewable energy capacity and doubling energy efficiency by 2030, Technical report, International Renewable Energy Agency.

Jenkins, Clinton N, Stuart L Pimm, and Lucas N Joppa, 2013, Global patterns of terrestrial vertebrate diversity and conservation, *Proceedings of the National Academy of Sciences* 110, E2602–E2610.

Kashyap, Shruti, Charles Mario Abela, Veronique Blum, and Beatrice Crona, 2025, Business and finance on a path towards meaningful biodiversity reporting?, *Current Opinion in Environmental Sustainability* 77, 101588.

Krueger, Philipp, Zacharias Sautner, and Laura T Starks, 2020, The importance of climate risks for institutional investors, *Review of Financial Studies* 33, 1067–1111.

Kruitwagen, Lucas, K.T. Story, J. Friedrich, L. Byers, S. Skillman, and Cameron Hepburn, 2021, A global inventory of photovoltaic solar energy generating units, *Nature* 598, 604–610.

Kwok, Tsz Chun, Daniel Spiro, and Arthur A. van Benthem, 2026, Firm ownership and pollution, *Journal of Environmental Economics and Management* 136, 103265.

Lammerant, Johan, Kim Driesen, Jolien Verhelst, and Jo De Ryck, 2022, Assessment of biodiversity measurement approaches for businesses and financial institutions—Update 4, Technical report, EU Business @ Biodiversity Platform, Brussels.

Li, Xuecao, Peng Gong, Yuyu Zhou, Jie Wang, Yuqi Bai, Bin Chen, Tengyun Hu, Yixiong Xiao, Bing Xu, Jun Yang, et al., 2020, Mapping global urban boundaries from the global artificial impervious area (GAIA) data, *Environmental Research Letters* 15, 094044.

Lopez, Anthony, Trieu Mai, Eric Lantz, Dylan Harrison-Atlas, Travis Williams, and Galen Maclaurin, 2021, Land use and turbine technology influences on wind potential in the United States, *Energy* 223, 120044.

Mair, Louise, Eduardo Amorim, Monira Bicalho, Thomas M. Brooks, Vincente Calfo, Renata de T. Capellão, Colin Clubbe, Marianne Evju, Eduardo P. Fernandez, Gláucia C Ferreira, et al., 2023, Quantifying and mapping species threat abatement opportunities to support national target setting, *Conservation Biology* 37, e14046.

Mair, Louise, Leon A. Bennun, Thomas M. Brooks, Stuart H.M. Butchart, Friederike C. Bolam, Neil D. Burgess, Jonathan M.M. Ekstrom, E.J. Milner-Gulland, Michael Hoffmann, Keping Ma, et al., 2021, A metric for spatially explicit contributions to science-based species targets, *Nature Ecology & Evolution* 5, 836–844.

Meng, Lina, Pengfei Liu, Yinggang Zhou, and Yingdan Mei, 2025, Blaming the wind? The impact of wind turbine on bird biodiversity, *Journal of Development Economics* 172, 103402.

Montesino Pouzols, Federico, Tuuli Toivonen, Enrico Di Minin, Aija S Kukkala, Peter Kullberg, Johanna Kuusterä, Joona Lehtomäki, Henrikki Tenkanen, Peter H Verburg, and Atte Moilanen, 2014, Global protected area expansion is compromised by projected land-use and parochialism, *Nature* 516, 383–386.

NextEnergy, 2025, Nature strategy & delivery framework, Technical report, NextEnergy Group.

Nvidia, 2025, Sustainability report: Fiscal year 2025, https://images.nvidia.com/aem-dam/Solutions/documents/NVIDIA-Sustainability-Report-Fiscal-Year-2025.pdf.

Pekel, Jean-François, Andrew Cottam, Noel Gorelick, and Alan S. Belward, 2016, High-resolution mapping of global surface water and its long-term changes, *Nature* 540, 418–422.

Potapov, Peter, Matthew C Hansen, Amy Pickens, Andres Hernandez-Serna, Alexandra Tyukavina, Svetlana Turubanova, Viviana Zalles, Xinyuan Li, Ahmad Khan, Fred Stolle, et al., 2022, The global 2000-2020 land cover and land use change dataset derived from the landsat archive: first results, *Frontiers in Remote Sensing* 3, 856903.

Schipper, Aafke M, Jelle P Hilbers, Johan R Meijer, Laura H Antão, Ana Benítez-López, Melinda MJ de Jonge, Luuk H Leemans, Eddy Scheper, Rob Alkemade, Jonathan C Doelman, et al., 2020, Projecting terrestrial biodiversity intactness with globio 4, *Global Change Biology* 26, 760–771.

Schneider, Julia M, Ruth Delzeit, Christian Neumann, Tobias Heimann, Ralf Seppelt, Franziska Schuenemann, Mareike Söder, Wolfram Mauser, and Florian Zabel, 2024, Effects of profit-driven cropland expansion and conservation policies, *Nature Sustainability* 7, 1335–1347.

Shive, Sophie A., and Margaret M. Forster, 2020, Corporate governance and pollution externalities of public and private firms, *Review of Financial Studies* 33, 1296–1330.

Stroebel, Johannes, and Xuran Zeng, 2025, Biodiversity vs. climate risk exposures of renewable energy firms, in Maximilian Auffhammer, Elías Albagli, Sofia Bauducco, and Gonzalo García-Trujillo, eds., *Implications of Climate Change and Ecosystem Services Degradation for Macroeconomic and Financial Stability*, volume 31, 185–202.

Thaker, Maria, Amod Zambre, and Harshal Bhosale, 2018, Wind farms have cascading impacts on ecosystems across trophic levels, *Nature Ecology & Evolution* 2, 1854–1858.

Visser, Elke, Vonica Perold, Samantha Ralston-Paton, Alvaro C Cardenal, and Peter G Ryan, 2019, Assessing the impacts of a utility-scale photovoltaic solar energy facility on birds in the Northern Cape, South Africa, *Renewable Energy* 133, 1285–1294.

Wang, Jingyu, Cai Li, Zhongci Deng, Jamie Carr, Lindsay C Stringer, Keke Li, Yuanchao Hu, Chen Zeng, Kai Huang, Sha Peng, et al., 2025, Biodiversity impacts of land occupation for renewable energy infrastructure in a globally connected world, *Environmental Science & Technology* 59, 9529–9539.

Zarfl, Christiane, Alexander E. Lumsdon, Jürgen Berlekamp, Laura Tydecks, and Klement Tockner, 2015, A global boom in hydropower dam construction, *Aquatic Sciences* 77, 161–170.

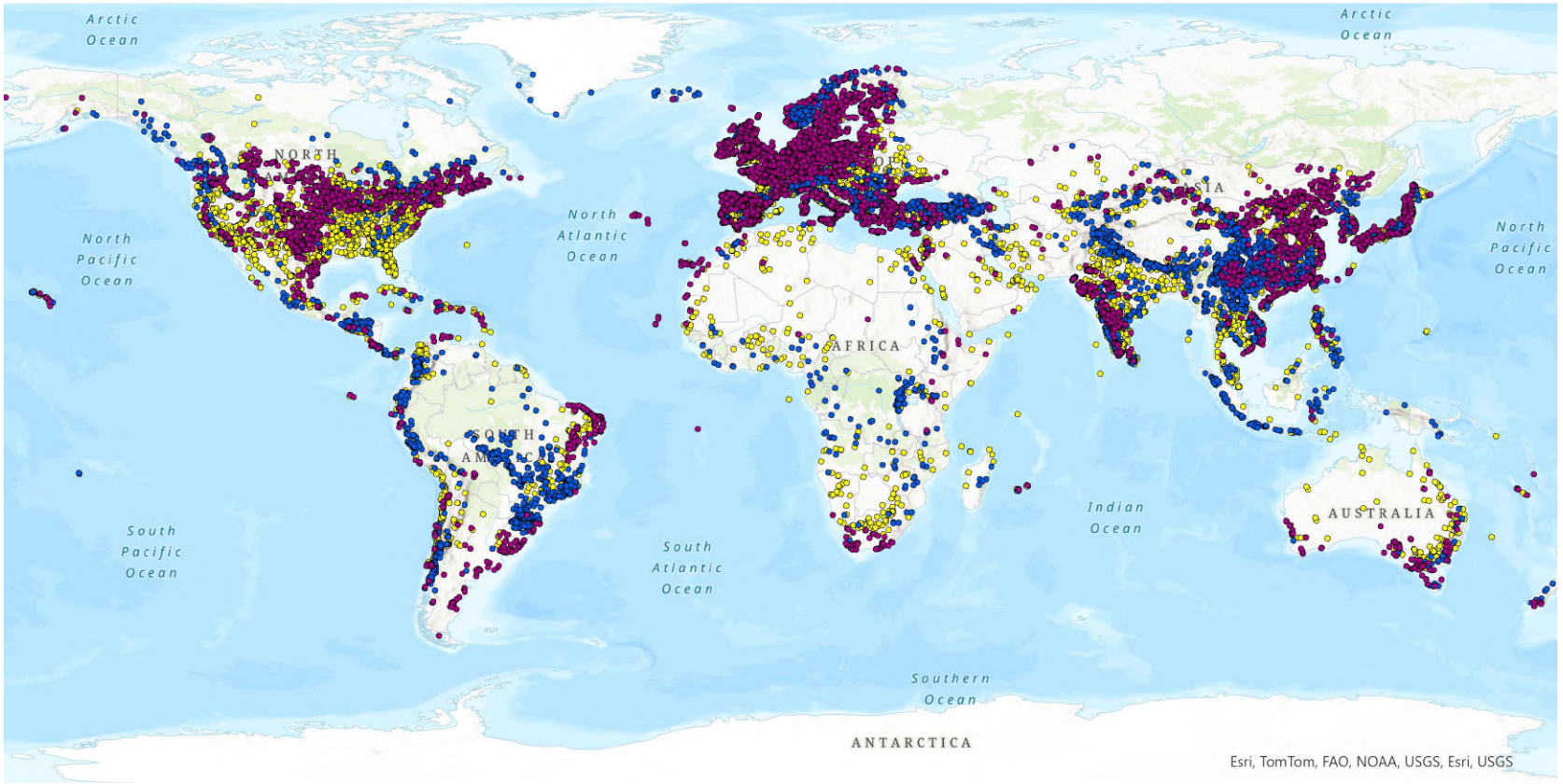
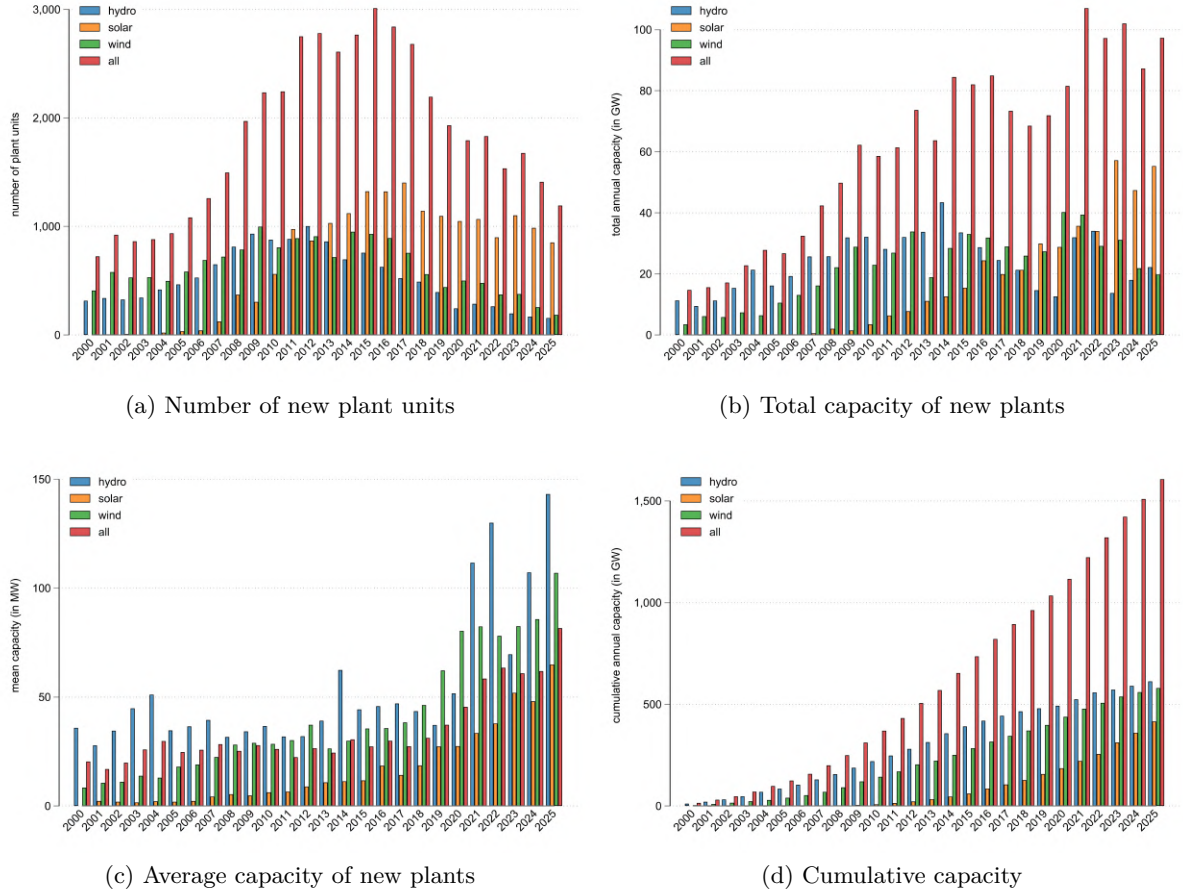


Figure 1: This figure shows the locations of solar (yellow), wind (purple), and hydro (blue) plant units included in the sample.



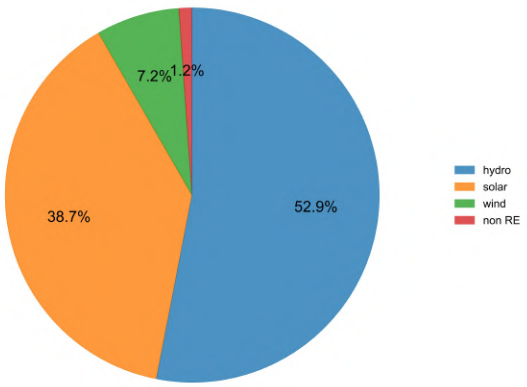
(a) Number of new plant units

(b) Total capacity of new plants

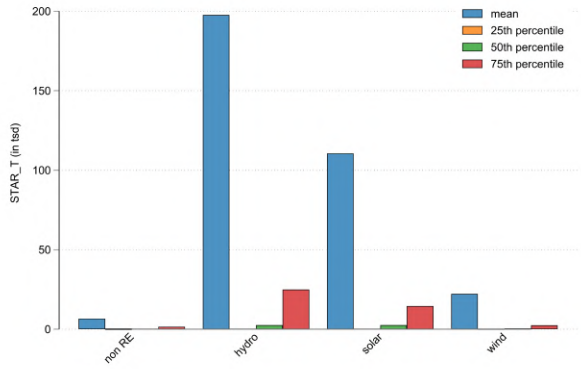
(c) Average capacity of new plants

(d) Cumulative capacity

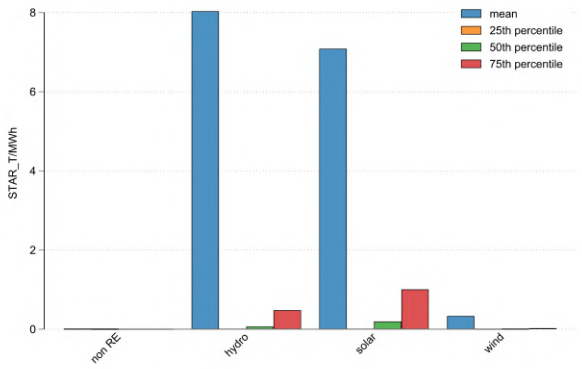
Figure 2: Panel (a) shows the number of new power plant units by technology and year. Panel (b) shows the total newly added capacity by year and technology. Panel (c) shows the average capacity of newly added plants by year and technology. Panel (d) shows the cumulative capacity by technology since 2000. Only power plant units included in our sample are considered.



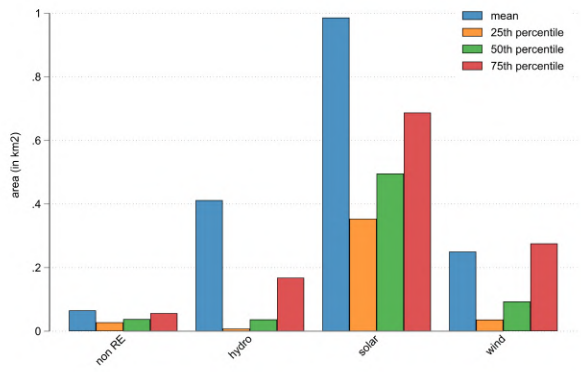
(a) Total STAR_T by technology



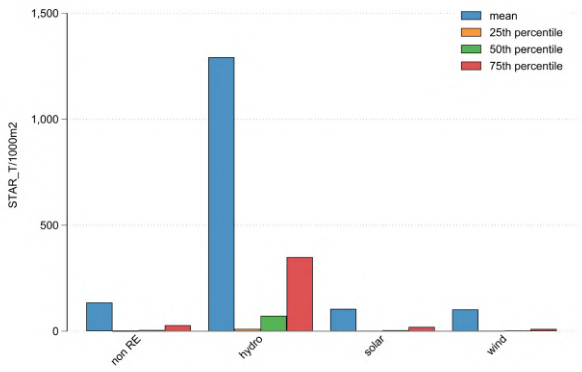
(b) STAR_T per plant



(c) STAR_T per MWh

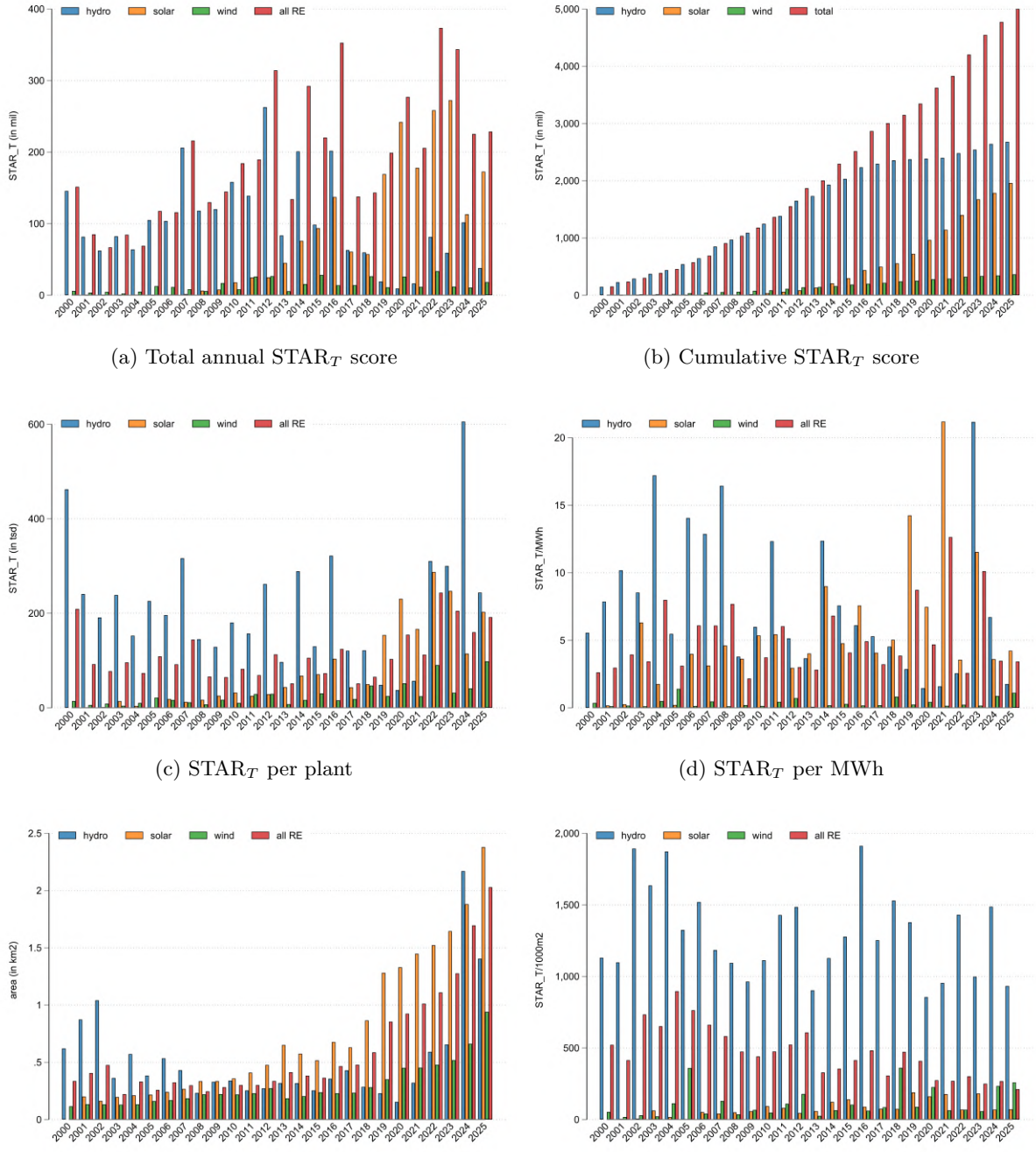


(d) Land use per plant in km^2



(e) STAR_T per 1,000 m^2

Figure 3: These figures show the land-use induced biodiversity impact of RE and non-RE plants by technology. Panel (a) shows how much plant units with different technologies contribute to the total STAR_T score. Panels (b) to (e) show, by technology, the mean, 25^{th}, 50^{th}, and 75^{th} percentile for (i) the STAR_T score per plant unit, (ii) the STAR_T score per MWh of expected generation, (iii) land use per plant unit (in km^2), and (iv) the STAR_T score per 1,000 m^2.



(a) Total annual STAR_T score

(b) Cumulative STAR_T score

(c) STAR_T per plant

(d) STAR_T per MWh

(e) Land use per plant in km^2

(f) STAR_T per 1,000 m^2

Figure 4: These figures show the biodiversity impacts of RE plant units over time. Panel (a) shows the total annual STAR_T score and Panel (b) the cumulative STAR_T score over time. Panels (c) to (f) show, by technology, the time-series of the mean of (i) the STAR_T score per plant unit, (ii) the STAR_T score per MWh of expected generation, (iii) land use per plant unit (in km^2), and (iv) the STAR_T score per 1,000 m^2.



Figure 5: This figure illustrates the counterfactual location choice within a 10 km radius, using the Ichigo Nago Futami Eco Power Plant as an example. The yellow point indicates the plant's actual location, while the red point marks the proposed counterfactual site 9.2 km away. Choosing the counterfactual site would reduces the STAR_T-based biodiversity impact from 19.1 million to 0.3 million, a 98.4% reduction.

Table 1: Plant-Level Quantification of Biodiversity Impacts of RE

	Obs.	Mean	p25	p50	p75	SD
STAR_T (thousand)	47,616	105.04	0.07	1.10	10.64	1,320.10
$\frac{\text{STAR}_T}{\text{MWh}}$	47,616	13.73	0.01	0.10	1.00	250.82
$\frac{\text{STAR}_T}{1{,}000\text{m}^2}$	47,615	442.32	0.92	7.44	53.49	3,421.93
Area (km^2)	47,616	0.57	0.04	0.22	0.51	1.67
Capacity (MW)	47,616	33.75	2.80	8.00	29.00	78.89
Generation (GWh)	47,616	98.14	7.49	22.34	82.20	238.90

This table presents summary statistics at the plant-unit level of the biodiversity impact of RE. We report the STAR_T score, the STAR_T intensity (STAR_T/MWh), and the STAR_T density (STAR_T/1,000m^2). We display the number of observations, mean, 25^{th} percentile, median, 75^{th} percentile, and standard deviation. The table additionally reports information on plant unit size, capacity, and expected generation. Variable definitions can be found in Appendix A.

Table 2: Top-10 Plants with the Highest Biodiversity Impact

Power Plant	Technology	Country	Year	Capacity (MW)	$\text{STAR}_{\boldsymbol{T}}$ (million)
Pachamama II Solar	Solar	Mexico	2020	330.0	120.8
El Cajon	Hydro	Mexico	2007	750.0	119.9
Mangilao Solar Plant	Solar	USA	2022	60.0	116.3
Metz Solar Plant	Solar	Australia	2022	115.0	80.3
Kamchay Hydroelectric	Hydro	Cambodia	2012	193.3	72.7
Central Hidroeléctrica URRÁ	Hydro	Colombia	2000	340.0	68.0
Tengger Desert Plant	Solar	China	2016	1,547.0	67.5
Central Hidroeléctrica Ituango	Hydro	Colombia	2022	2,400.0	61.4
Aldea Blanca Planta Solar	Solar	Spain	2021	9.2	56.0
Konal Hydro Plant	Hydro	India	2010	10.0	55.6

This table shows the ten RE plants with the highest STAR_T score. We sort the plants based on the STAR_T score. Year is the year in which commercial operation started. Variable definitions can be found in Appendix A.

Table 3: Aggregate Quantification of Biodiversity Impacts of RE

	$STAR_T$ (billion)			
	Hydro	Solar	Wind	Total
Current Impact				
Biodiversity Impact of Existing Plants	2.68	1.96	0.36	5.00
Scenario 1: Mid-Term				
Including Impact from Planned Plants	3.05	3.32	1.05	7.42
Scenario 2: Mid-Term				
Including Impact from Capacity Forecasts until 2030	3.25	10.11	0.74	14.10
Scenario 3: Long-Term				
Including Impact from Capacity Forecasts until 2050	5.55	44.81	2.65	53.01

This table quantifies the biodiversity impact of existing and future RE plant units using different scenarios. For calculating the current impact, we include in the calculation all existing RE power plant units from the S&P MI database that went into operation between 2000 and 2025. In Scenario 1, we add to the currently existing plant units those that are planned (RE plants with the status "planned" in the S&P MI database as of Q1 2026) and then calculate the impact from existing and planned plant units. In Scenario 2, we instead add to the current biodiversity impacts those implied by forecasted capacity changes until 2030 based on data from the IEA's Renewable Energy Progress Tracker. In Scenario 3, we instead add to the current impacts the impacts implied by additional RE capacity as derived from the 2050 generation forecast from the IEA's World Energy Outlook 2025. For this scenario, we convert generation forecasts into capacity predictions based on technology-specific capacity factors from the IEA. In Scenario 1, we calculate $STAR_T$ values using their planned locations. In Scenarios 2 and 3, which are based on forecasted capacities, we estimate $STAR_T$ values by multiplying the forecasted capacities with the average $STAR_T$ scores per unit of capacity of existing RE plants with the same technology. Variable definitions can be found in Appendix A.

Table 4: Biodiversity Impacts across Technologies and Time

Panel A: Biodiversity Impacts across Technologies

	Log(STAR_T)			Log($\frac{\text{STAR}_T}{\text{MWh}}$)	Log($\frac{\text{STAR}_T}{1{,}000\text{m}^2}$)
	(1)	(2)	(3)	(4)	(5)
Solar	2.34***	2.65***	5.80***	7.00***	0.057
	(36.9)	(41.9)	(71.1)	(114)	(0.98)
Wind	-0.31***	1.20***	3.33***	4.15***	-0.044
	(-4.52)	(18.5)	(46.4)	(67.6)	(-0.75)
Hydro	2.13***	1.84***	4.50***	5.51***	2.01***
	(28.4)	(25.6)	(52.4)	(79.1)	(32.7)
Log(Generation)			0.72***		
			(57.3)		
Observations	52,918	52,900	52,900	52,900	52,900
Adj. R^2	0.14	0.44	0.51	0.60	0.48
Country FE	No	Yes	Yes	Yes	Yes
Year FE	No	Yes	Yes	Yes	Yes

Panel B: Biodiversity Impacts over Time

	Log(STAR_T)			Log($\frac{\text{STAR}_T}{\text{MWh}}$)	Log($\frac{\text{STAR}_T}{1{,}000\text{m}^2}$)
	(1)	(2)	(3)	(4)	(5)
Year COD	0.11***	0.043***	-0.0027	-0.021***	0.0042*
	(32.3)	(12.9)	(-0.85)	(-6.51)	(1.67)
Log(Generation)			0.72***		
			(56.0)		
Observations	44,441	44,418	44,418	44,418	44,418
Pseudo/Adj. R^2	0.047	0.44	0.52	0.48	0.51
Country FE	No	Yes	Yes	Yes	Yes
Technology FE	No	Yes	Yes	Yes	Yes

continued on next page

Table 4 continued

Panel C: Biodiversity Impacts and RE Penetration

	Log($STAR_T$)			Log($\frac{STAR_T}{MWh}$)	Log($\frac{STAR_T}{1{,}000m^2}$)
	(1)	(2)	(3)	(4)	(5)
Share $RE^{t-3}_{Country}$	1.00***	1.78***	1.45***	1.31***	0.57*
	(8.83)	(3.54)	(3.11)	(2.76)	(1.73)
Log(Generation)			0.71***		
			(55.1)		
Observations	44,381	44,369	44,369	44,369	44,369
Pseudo/Adj. R^2	0.0041	0.45	0.52	0.48	0.51
Country FE	No	Yes	Yes	Yes	Yes
Year FE	No	Yes	Yes	Yes	Yes
Technology FE	No	Yes	Yes	Yes	Yes

This table relates the biodiversity impact of RE plant units to their technologies, start of commercial operation, and degree of penetration of RE in a country. The dependent variables measure the biodiversity impacts of plant units and are indicated in each column. In Panel A, the key independent variables are Solar, Wind, and Hydro, which are dummy variables that each equal one for solar, wind, and hydro plant units, respectively. Non-RE plant units (i.e., fossil-fuel and nuclear plants) are omitted and serve as the baseline category. In Panel B, the key independent variable is Year COD, which is defined as the year in which commercial operation started. In Panel C, the key independent variable is Share $RE^{t-3}_{Country}$, which captures RE penetration and is calculated as the share of RE capacity relative to the total generation capacity in a country. This variable is measured three years before the start of commercial operation of the plant unit. Year fixed effects are based on the plant unit's start year of commercial operation, country fixed effects are based on the country in which it is located, and technology fixed effects are based on its generation technology. Regressions are estimated at the plant-unit level. The number of observations changes from Column (1) to Columns (2) to (5) because some countries with only one power plant unit are dropped with country fixed effects. *t*-statistics based on robust standard errors clustered by power plants are presented in parentheses. ***, ** and * indicate significance at the 1%-, 5%- and 10%-levels, respectively. Variable definitions can be found in Appendix A.

Table 5: Variation and Concentration of Plant-level Biodiversity Impacts

Panel A: Coefficient of Variation across Plants

	CV(STAR_T)	CV($\frac{(\text{STAR}_T}{\text{MWh}}$)	CV($\frac{\text{STAR}_T}{1{,}000\text{m}^2}$)
Overall	12.57	17.31	7.74
Within Technology	11.52	17.34	12.37
Within Year	9.90	12.58	7.55
Within Country	8.69	8.97	4.19
Within State	2.81	3.18	1.97
Within Region	1.51	1.62	0.95
Within Technology/Year/Country	3.22	3.14	2.57
Within Technology/Year/State	1.36	1.24	1.12
Within Technology/Year/Region	0.74	0.63	0.56

Panel B: Concentration within Top Plants

	STAR_T Share	Capacity Share	$\frac{\text{Capacity Share}}{\text{STAR}_T\text{Share}}$
Top-10 Plant Units	13.2%	0.2%	1.5%
Top-100 Plant Units	40.9%	0.8%	2.0%
Top-500 Plant Units	68.6%	3.1%	4.5%
Top-1% Plant Units	67.9%	2.9%	4.3%
Top-5% Plant Units	88.7%	12.4%	14.0%
Top-10% Plant Units	94.7%	24.4%	25.7%

Panel A shows the average coefficient of variation (CV) for different measures of the biodiversity impact of RE plant units (reported horizontally). The CV is the standard deviation divided by the mean. We report vertically the CVs calculated across all plant units, only plant units with the same technology, plant units that began commercial operation in the same year, plant units within the same country, state, or region, and plant units with the same technology that began commercial operation in the same year and within either the same country, state, or region. States are based on Administrative Level 1 boundaries (i.e., the largest subnational division of a country, such as states in the U.S.). Regions are based on Administrative Level 2 boundaries (i.e., the second-tier subnational division of a country, such as counties in the U.S.). Panel B shows the share of the total STAR_T score and total RE capacity that is attributable to the top-10/top-100/top-500 RE plant units or the top-1%/top-5%/top-10% of the RE plant units with the highest biodiversity impact. Capacity Share/STAR_T Share is the capacity share divided by the STAR_T share (with some rounding differences). Observations are at the plant-unit level. Variable definitions can be found in Appendix A.

Table 6: Counterfactual Siting for Wind/Solar Plants

	$STAR_T$ Reduction Relative to:		
	$STAR_T$ Score of Affected Plants	$STAR_T$ Score of All Solar/Wind Plants	$STAR_T$ Score of All RE Plants
	(1)	(2)	(3)
Panel A: Counterfactual Locations within 10 km Radius			
Top-1% Plant Units	86.2%	55.1%	25.6%
Top-5% Plant Units	81.3%	69.5%	32.3%
Top-10% Plant Units	79.5%	73.9%	34.3%
Panel B: Counterfactual Locations within 20 km Radius			
Top-1% Plant Units	91.3%	60.2%	27.9%
Top-5% Plant Units	88.8%	77.1%	35.8%
Top-10% Plant Units	87.9%	82.4%	38.2%
Panel C: Counterfactual Locations within 50 km Radius			
Top-1% Plant Units	94.6%	63.5%	29.5%
Top-5% Plant Units	94.0%	82.3%	38.2%
Top-10% Plant Units	93.7%	88.2%	40.9%

This table shows estimates of the potential biodiversity impact reduction if alternative sitings with a lower biodiversity impact would have been chosen for the highest-impact wind and solar plant units. We consider a radius of 10 km (Panel A), 20 km (Panel B), or 50 km (Panel C) around the actual location of a plant unit for the counterfactual siting. Specifically, we choose an equally-sized area with the lowest $STAR_T$ value within a given radius as the counterfactual siting. Only locations where construction is possible are considered (see Internet Appendix IA.G for details). The potential impact reduction is then calculated as the percentage difference between a plant unit's actual $STAR_T$ value and the $STAR_T$ value that the plant unit would have had at the counterfactual location. Potential reductions are analyzed for the top-1%/top-5%/top-10% of solar and wind plant units with the highest biodiversity impact. Column (1) reports the potential total $STAR_T$ score reduction in percent for all considered plant units (e.g., the top-1%). Column (2) reports the value of the $STAR_T$ reduction relative to the $STAR_T$ value of all wind and solar plant units. Column (3) reports the the same reduction relative to the total biodiversity impact of all RE plant units, including hydro plant units. All statistics are calculated at the plant-unit level. Variable definitions can be found in Appendix A.

Table 7: Variation and Concentration of Firm-level Biodiversity Impacts

Panel A: Coefficient of Variation across Firms

	CV(STAR_T)	CV($\frac{\text{STAR}_T}{\text{MWh}}$)	CV($\frac{\text{STAR}_T}{1{,}000\text{m}^2}$)
Overall	9.48	15.52	6.76
Within Technology	8.19	12.87	8.73
Within Year	10.21	11.46	7.53
Within Country	5.69	5.84	2.86
Within State	2.64	2.42	1.67
Within Region	1.66	1.36	0.89
Within Technology/Year/Country	2.68	2.41	1.97
Within Technology/Year/State	1.48	1.05	0.94
Within Technology/Year/Region	1.08	0.59	0.52

Panel B: Concentration within Top Firms

	STAR_T Share	Capacity Share	$\frac{\text{Capacity Share}}{\text{STAR}_T\text{Share}}$
Top-10 Firms	18.1%	0.6%	3.1%
Top-100 Firms	58.6%	10.9%	18.7%
Top-500 Firms	85.0%	37.2%	43.8%
Top-1% Firms	65.6%	14.9%	22.7%
Top-5% Firms	89.6%	44.5%	49.6%
Top-10% Firms	95.8%	59.4%	62.0%

Panel A shows the average coefficient of variation (CV) of the firms (identified as the direct owners) behind RE plants for different measures of the biodiversity impact of RE (reported horizontally). The CV is the standard deviation divided by the mean. For the overall CV reported in the first line, we calculate the sum of the STAR_T score, and the average values of $\frac{\text{STAR}_T}{\text{MWh}}$ and $\frac{\text{STAR}_T}{1{,}000\text{m}^2}$, across all plants of a firm. For the lines below, we only consider firms' plants with the same technology, plants that began commercial operation in the same year, plants within the same country, state, or region, and plants with the same technology that began commercial operation in the same year and within either the same country, state, or region. The standard deviation is then calculated based on the standard deviation of this firm-specific sum or mean. For the "within" CVs, we report the average CV across all groups in the table. States are based on Administrative Level 1 boundaries (i.e., the largest subnational division of a country, such as states in the U.S.). Regions are based on Administrative Level 2 boundaries (i.e., the second-tier subnational division of a country, such as counties in the U.S.). Panel B shows the share of the total STAR_T score and of the total RE capacity that is attributable to the top-10/top-100/top-500 firms or the top-1%/top-5%/top-10% of firms (identified as the direct owners) of RE plants with the highest biodiversity impact. Capacity Share/STAR_T Share is simply the capacity share divided by the STAR_T share (with some rounding differences). Observations are at the firm-plant-unit level. Variable definitions can be found in Appendix A.

Table 8: Ownership by Unlisted versus Listed Firms

Panel A: Overall Effect				
	$\text{Log}(\text{STAR}_T)$		$\text{Log}(\frac{\text{STAR}_T}{\text{MWh}})$	$\text{Log}(\frac{\text{STAR}_T}{1{,}000\text{m}^2})$
	(1)	(2)	(3)	(4)
$\text{Listing}_{\text{Direct/Ultimate}}$	0.56***	0.026	-0.0061	0.020
	(6.55)	(1.29)	(-0.31)	(1.13)
Log(Generation)		0.94***		
		(152)		
Observations	68,509	68,509	68,509	68,509
Adj. R^2	0.71	0.88	0.83	0.84
Region × Technology FE	Yes	Yes	Yes	Yes
Year × Technology FE	Yes	Yes	Yes	Yes
Panel B: Within-Ultimate Parent Effect				
	$\text{Log}(\text{STAR}_T)$		$\text{Log}(\frac{\text{STAR}_T}{\text{MWh}})$	$\text{Log}(\frac{\text{STAR}_T}{1{,}000\text{m}^2})$
	(1)	(2)	(3)	(4)
$\text{Listing}_{\text{Direct}}$	-0.20***	-0.092**	-0.076*	-0.048
	(-2.90)	(-2.09)	(-1.74)	(-1.22)
Log(Generation)		0.87***		
		(80.3)		
Observations	62,655	62,655	62,655	62,655
Adj. R^2	0.86	0.90	0.86	0.86
Region × Technology FE	Yes	Yes	Yes	Yes
Year × Technology FE	Yes	Yes	Yes	Yes
Parent × Year FE	Yes	Yes	Yes	Yes

This table relates the biodiversity impact of RE plant units to whether the owner is listed or unlisted. The dependent variables measure the biodiversity impacts of different plant units and are indicated in each column. $\text{Listing}_{\text{Direct/Ultimate}}$ equals one if either the direct or ultimate owner of the power plant unit is listed on a public exchange, and zero otherwise. $\text{Listing}_{\text{Direct}}$ equals one if the direct owner of the power plant unit is listed at a public exchange, and zero otherwise. Year fixed effects are based on the plant's start year of commercial operation and technology fixed effects are based on its generation technology. Region fixed effects are based on Administrative Level 2 boundaries. Parent fixed effects are based on the ultimate parent of the direct owner of the plant. Regressions are estimated at the plant-unit-owner level. *t*-statistics based on robust standard errors clustered by the plant units' ultimate parents are presented in parentheses. ***, ** and * indicate significance at the 1%-, 5%- and 10%-levels, respectively. Variable definitions can be found in Appendix A.

Table 9: Ownership by Financial versus Non-Financial Firms

Panel A: Overall Effect

	$\text{Log}(\text{STAR}_T)$		$\text{Log}(\frac{\text{STAR}_T}{\text{MWh}})$	$\text{Log}(\frac{\text{STAR}_T}{1{,}000\text{m}^2})$
	(1)	(2)	(3)	(4)
$\text{Financial Owner}_{\text{Direct/Ultimate}}$	-0.45***	-0.080***	-0.057**	-0.032
	(-3.12)	(-2.87)	(-2.13)	(-1.43)
Log(Generation)		0.94***		
		(151)		
Observations	67,899	67,899	67,899	67,899
Adj. R^2	0.71	0.88	0.83	0.84
Region × Technology FE	Yes	Yes	Yes	Yes
Year × Technology FE	Yes	Yes	Yes	Yes

Panel B: Within-Ultimate Parent Effect

	$\text{Log}(\text{STAR}_T)$		$\text{Log}(\frac{\text{STAR}_T}{\text{MWh}})$	$\text{Log}(\frac{\text{STAR}_T}{1{,}000\text{m}^2})$
	(1)	(2)	(3)	(4)
$\text{Financial Owner}_{\text{Direct}}$	-0.29	-0.22***	-0.21***	-0.12*
	(-1.64)	(-2.87)	(-2.67)	(-1.80)
Log(Generation)		0.87***		
		(80.4)		
Observations	62,655	62,655	62,655	62,655
Adj. R^2	0.86	0.90	0.86	0.86
Region × Technology FE	Yes	Yes	Yes	Yes
Year × Technology FE	Yes	Yes	Yes	Yes
Parent × Year FE	yes	Yes	Yes	Yes

This table relates the biodiversity impact of RE plant units to whether the owner is a financial or non-financial entity. The dependent variables measure the biodiversity impacts of different plant units and are indicated in each column. $\text{Financial Owner}_{\text{Direct/Ultimate}}$ equals one if either the direct or ultimate owner of the power plant unit is classified as a bank, endowment fund, hedge fund, insurance company, mutual fund, PE fund, or pension fund, and zero otherwise. $\text{Financial Owner}_{\text{Direct}}$ only considers direct owners for the classification. Year fixed effects are based on the plant's start year of commercial operation and technology fixed effects are based on its generation technology. Region fixed effects are based on Administrative Level 2 boundaries. Parent fixed effects are based on the ultimate parent of the direct owner of the plant. Regressions are estimated at the plant-unit-owner level. *t*-statistics based on robust standard errors clustered by the plant units' ultimate parents are presented in parentheses. ***, ** and * indicate significance at the 1%-, 5%- and 10%-levels, respectively. Variable definitions can be found in Appendix A.

Table 10: Project versus Corporate Financing

Panel A: Overall Effect

	Log($STAR_T$)		Log($\frac{STAR_T}{MWh}$)	Log($\frac{STAR_T}{1{,}000m^2}$)
	(1)	(2)	(3)	(4)
Project Financed	0.16***	0.068**	0.067**	0.092***
	(2.67)	(2.01)	(1.98)	(3.15)
Log(Generation)		0.99***		
		(161)		
Observations	42,503	42,503	42,503	42,503
Adj. R^2	0.73	0.91	0.86	0.87
Region × Technology FE	Yes	Yes	Yes	Yes
Year × Technology FE	Yes	Yes	Yes	Yes

Panel B: Within-Ultimate Parent Effect

	Log($STAR_T$)		Log($\frac{STAR_T}{MWh}$)	Log($\frac{STAR_T}{1{,}000m^2}$)
	(1)	(2)	(3)	(4)
Project Financed	0.22***	0.082**	0.077**	0.100***
	(4.21)	(2.11)	(2.00)	(2.91)
Log(Generation)		0.97***		
		(96.4)		
Observations	39,786	39,786	39,786	39,786
Adj. R^2	0.88	0.93	0.88	0.89
Region × Technology FE	Yes	Yes	Yes	Yes
Year × Technology FE	Yes	Yes	Yes	Yes
Parent × Year FE	Yes	Yes	Yes	Yes

This table relates the biodiversity impact of RE plant units to whether they are project or corporate financed. The dependent variables measure the biodiversity impacts of different plant units and are indicated in each column. Project Financed equals one if the power plant unit is project financed (off-balance sheet), and zero if it is corporate financed (on-balance sheet). Year fixed effects are based on the plant's start year of commercial operation and technology fixed effects are based on its generation technology. Region fixed effects are based on Administrative Level 2 boundaries. Parent fixed effects are based on the ultimate parent of the direct owner of the plant. Regressions are estimated at the plant-unit-owner level. *t*-statistics based on robust standard errors clustered by the plant units' ultimate parents are presented in parentheses. ***, ** and * indicate significance at the 1%-, 5%- and 10%-levels, respectively. Variable definitions can be found in Appendix A.

Internet Appendix

for

Biodiversity Impacts of Renewable Energy

Table of Contents

- Internet Appendix IA.A: Additional Tables and Figures
- Internet Appendix IA.B: Comparison of STAR Metric to Other Measures
- Internet Appendix IA.C: Details about STAR Estimation for Small Solar Plants
- Internet Appendix IA.D: Details about STAR Estimation for Fossil/Nuclear Plants
- Internet Appendix IA.E: Details about STAR Estimation for Planned Power Plants
- Internet Appendix IA.F: Details about Artificial Land Identification
- Internet Appendix IA.G: Details about Counterfactual Calculation

IA.A. Additional Tables and Figures

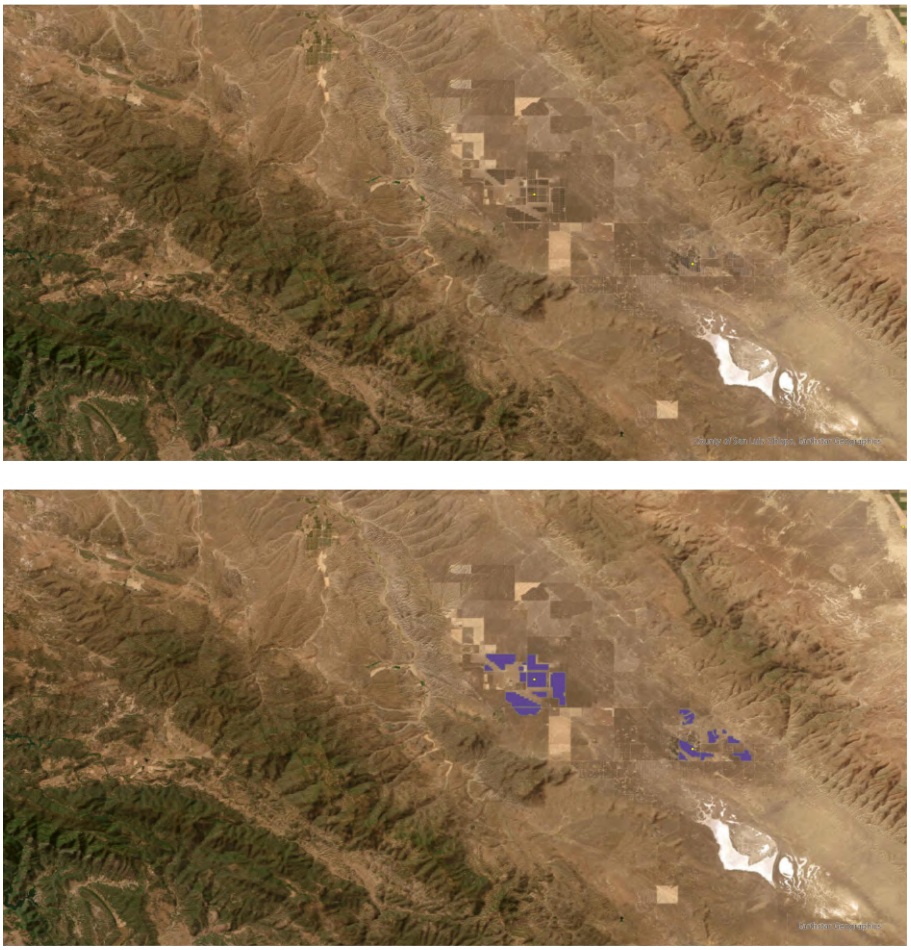


Figure IA.A.1: These figures illustrate the detection of the land-use footprint of a solar plant using Sentinel-2 satellite data. The plant is the Topaz Solar Farm in California, U.S., with a capacity of 129 MW. The top picture shows the original satellite image. The bottom picture illustrates the plant detection algorithm, with the plant's land-use footprint colored in purple.

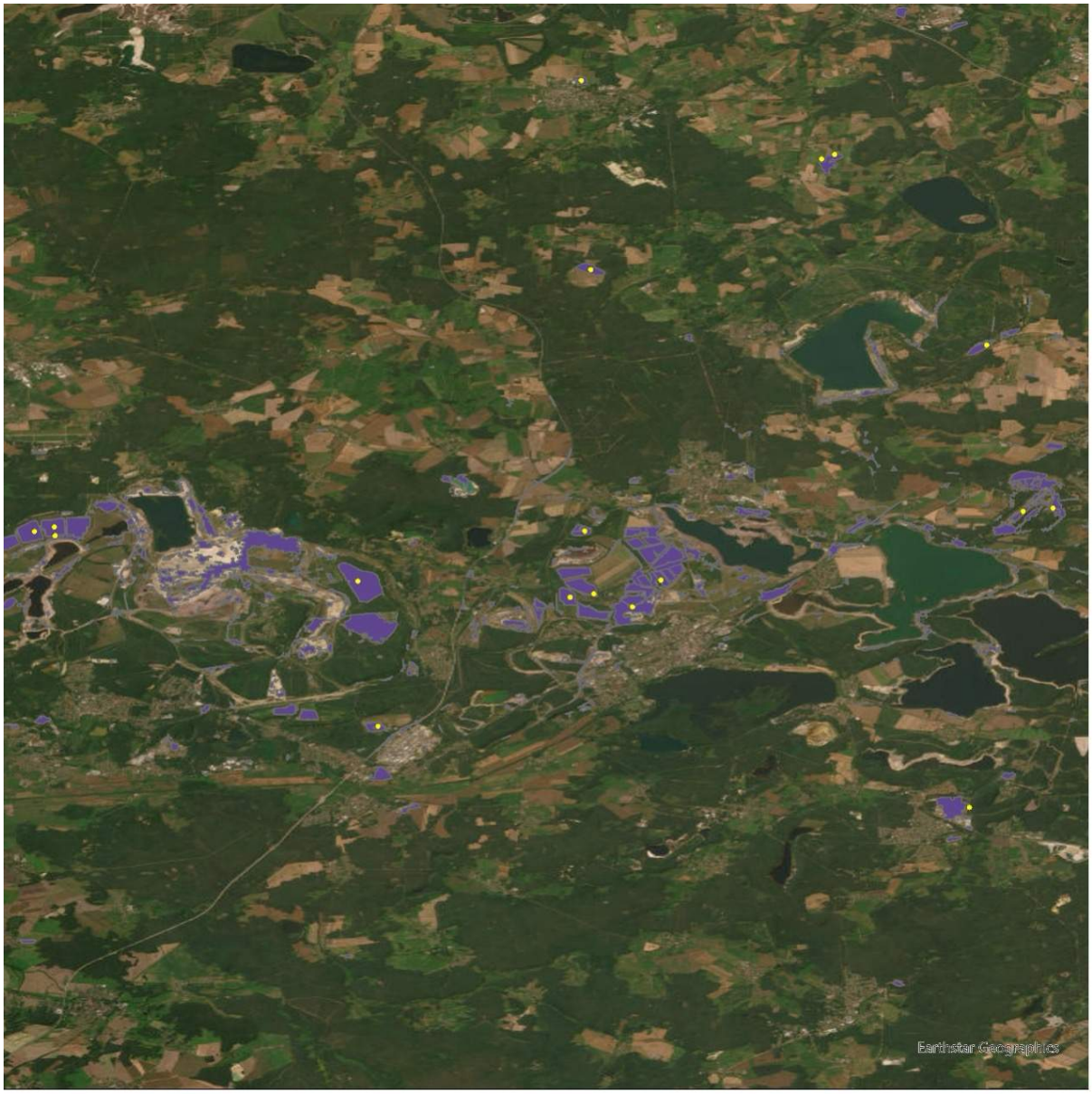


Figure IA.A.2: This figure shows land use footprints of solar plants near Königsberg, Germany. This example illustrates our methodology for handling clusters of plants, where we first calculate the overall land use of all closely-sited facilities and then allocated it to individual plants based on their capacities.

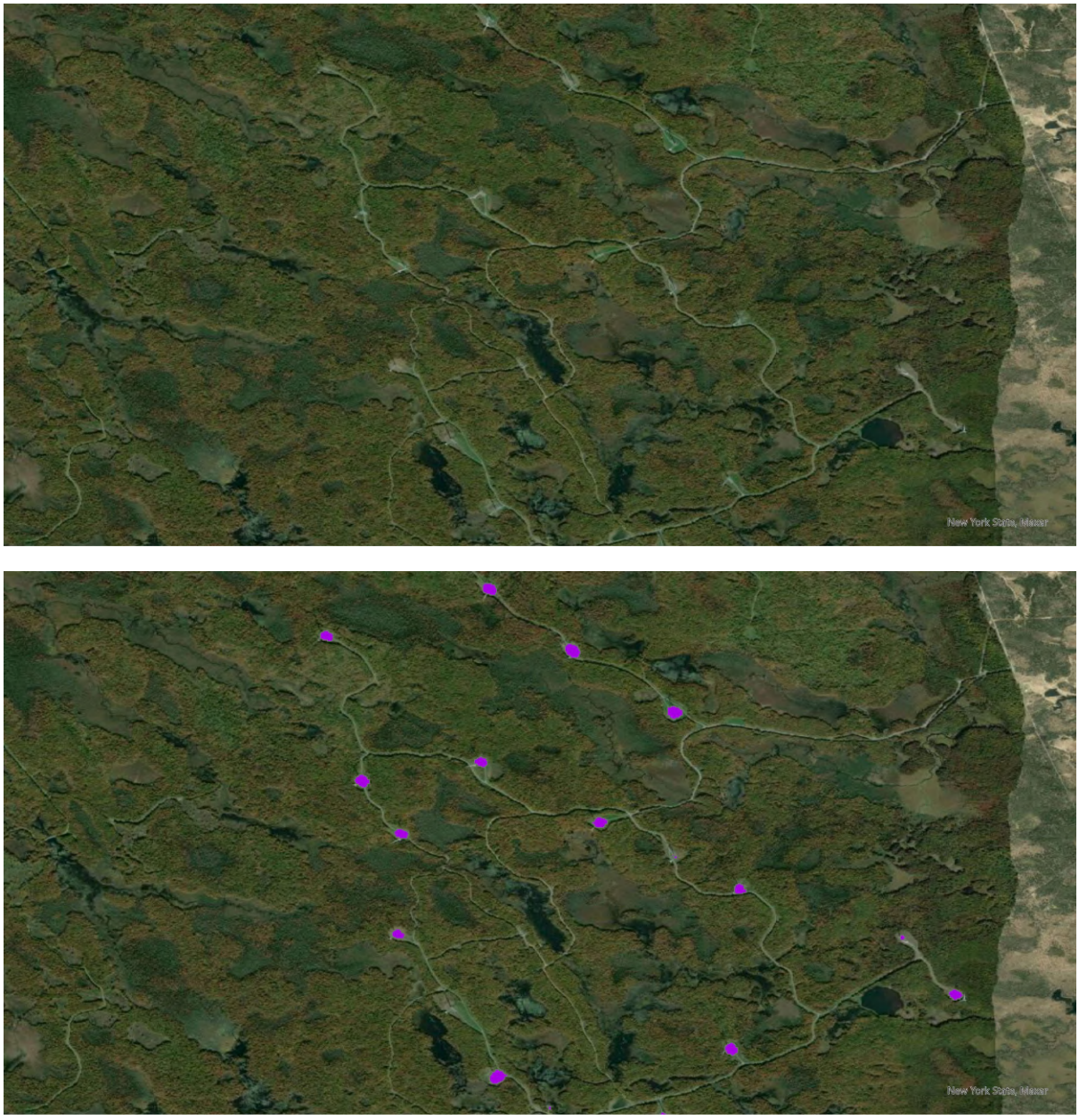


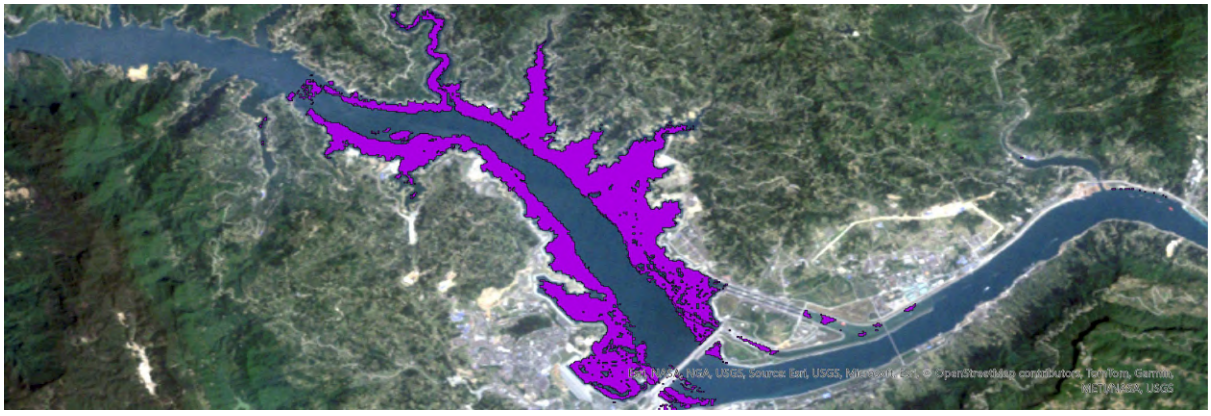
Figure IA.A.3: These figures illustrate the detection of the land-use footprint of a wind plant using Sentinel-2 satellite data. The plant is the Roaring Brook Wind Farm in New York State, U.S., with a capacity of 79.7 MW. The top picture shows the original satellite image. The bottom picture illustrates the plant detection algorithm, with the wind turbines colored in purple.



(a) original image - before dam construction



(b) original image - after dam construction



(c) plant detection algorithm

Figure IA.A.4: These figures illustrate the detection of the land-use footprint of a hydro plant using Sentinel-2 satellite data. The plant is the Three Gorges Dam in China with a capacity of 22,820 MW. The top picture shows the original satellite image before the dam was constructed. The middle picture shows the original satellite image after the dam was constructed. The bottom picture illustrates the plant detection algorithm, with the area affected by the hydro plant colored in purple.



(a) Dalate Steam Plant (Coal) in Dalate, China



(b) Ostrovets Nuclear Power Plant in Astravyets, Belarus



(c) Ceredo Power Plant (Gas) in Ceredo, USA



(d) Energypac Internal Combustion Plant (Oil) in Patiya, Bangladesh

Figure IA.A.5: This figure illustrates the manually delineated land-use boundaries of fossil-fuel based power plants. The examples are a 4,180 MW coal-fired plant in China, a 2,388 MW nuclear plant in Belarus, a 519 MW gas-fired plant in the U.S., and a 108 MW gas-fired plant in Bangladesh.

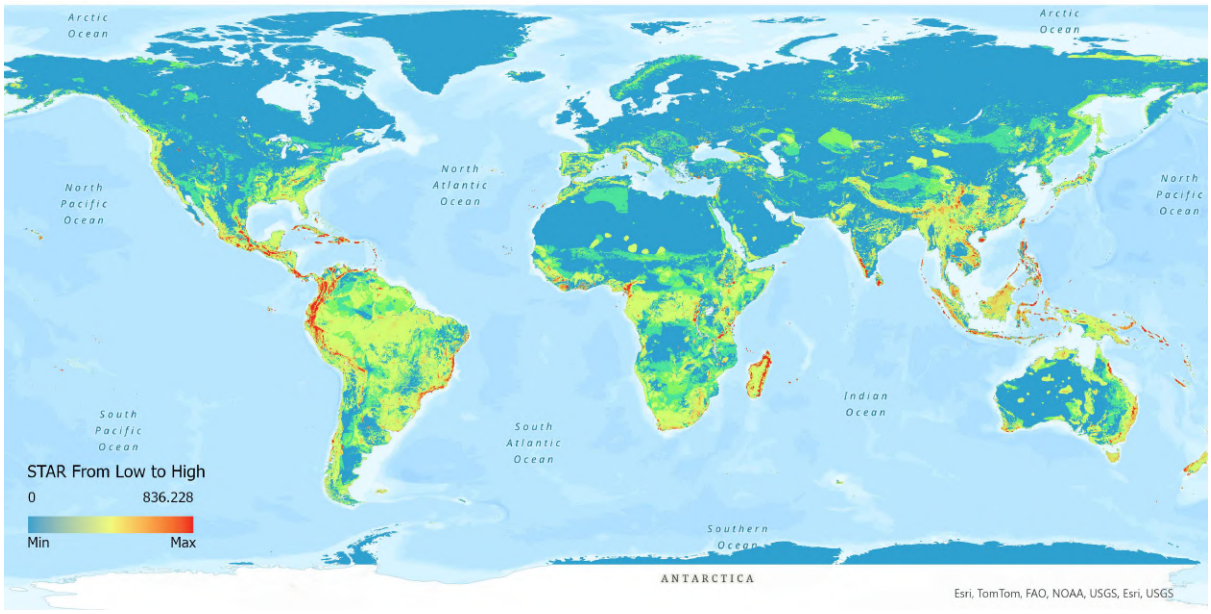


Figure IA.A.6: This figure illustrates variation in STAR_T scores around the world. Blue represents areas with low, and red areas with high, STAR_T scores.

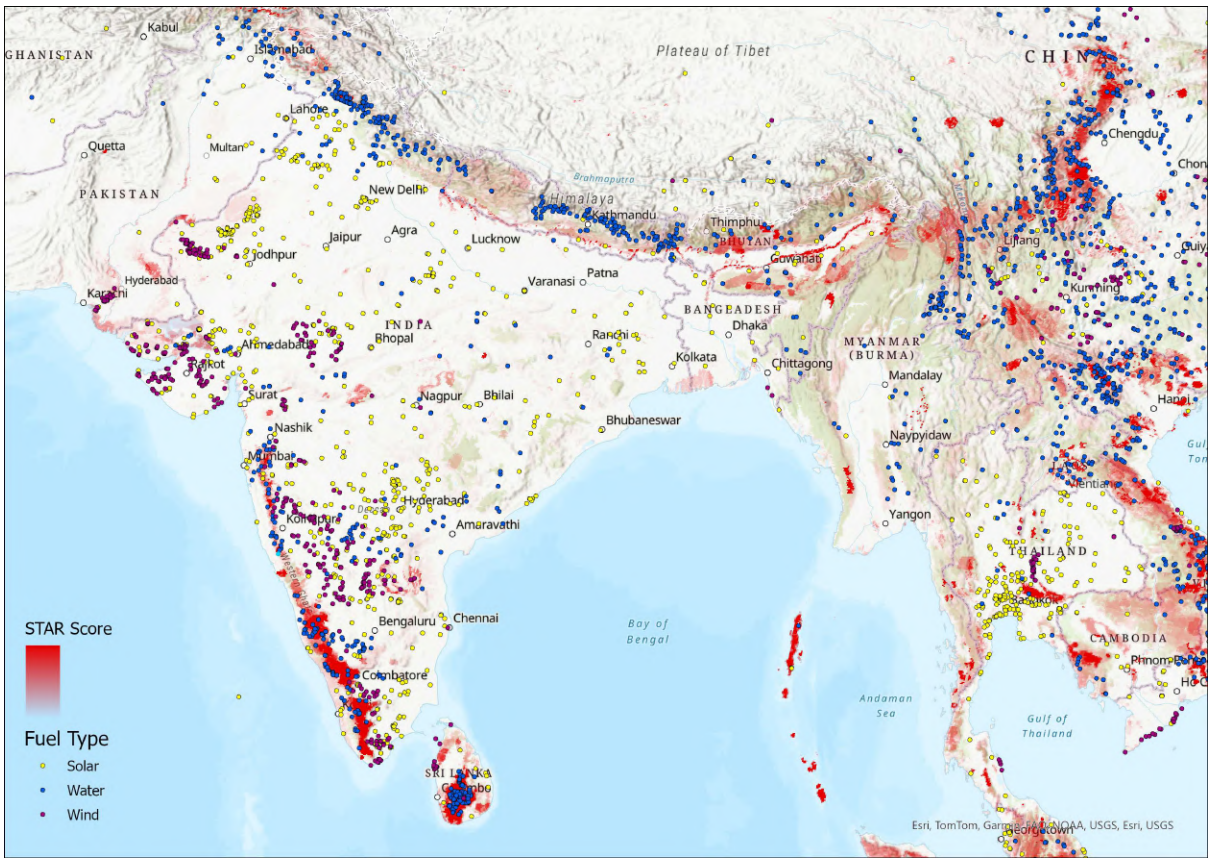


Figure IA.A.7: This figure illustrates the spatial relationship between RE plant units and STAR_T scores in South Asia. Solar plant units are in yellow, wind plant units in purple, and hydro plant units in blue. Areas with high STAR_T scores are colored in red.



Figure IA.A.8: This figure illustrates the area of habitat for the Nelson's Antelope Squirrel as well as the locations of RE power plants in California.

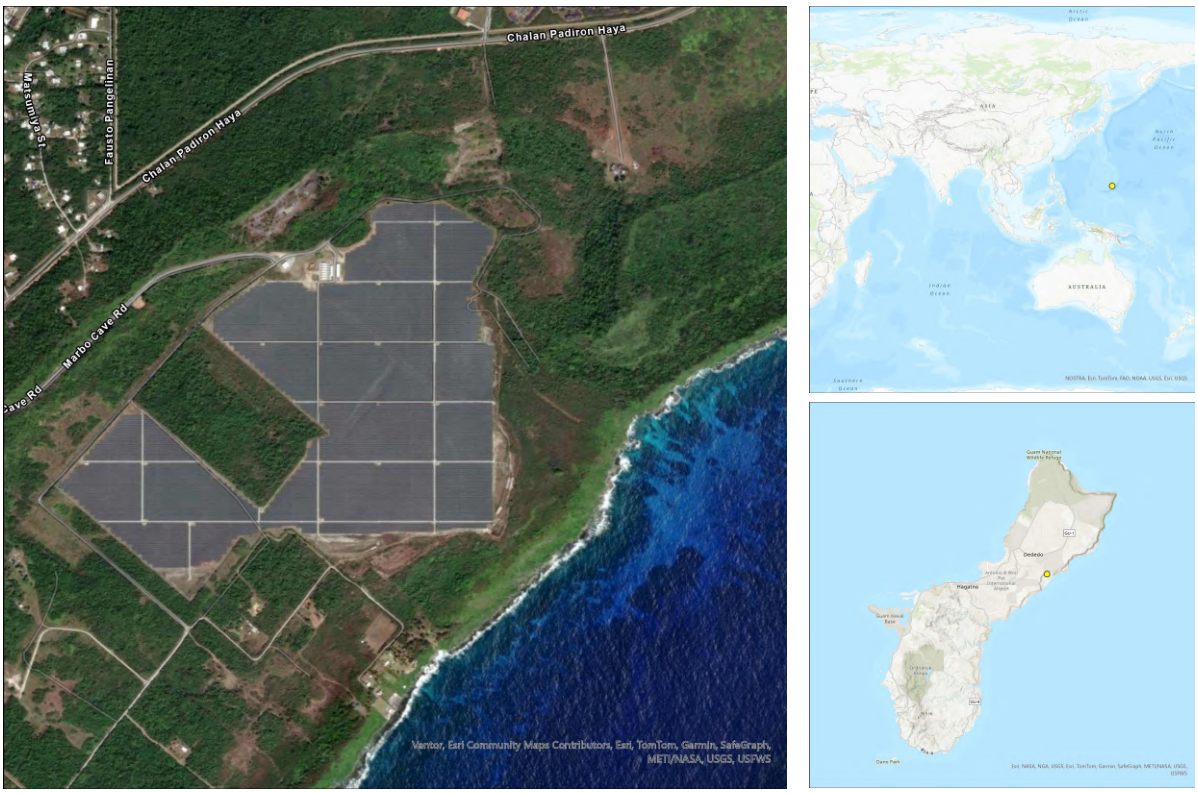


Figure IA.A.9: These figures illustrate the location of the Mangilao Solar Plant in Guam. The picture on the left is a satellite image of the plant and the pictures on the right are maps on which the plant's location is indicated with a yellow dot.



Figure IA.A.10: This figure illustrates the location of the Jinchang Jinchuan Solar Plant in the Gobi Desert. The picture on the left is a satellite image of the plant and the pictures on the right side are maps on which the plant's location is indicated with a yellow dot.

Table IA.A.1: Evidence on Land Use of RE Plants

Land type	Hydro	Solar	Wind	Total
Panel A: Total Land Use (in km2)				
Artificial	515.0	2,395.6	278.7	3,189.3
Bare	356.1	3,981.4	375.4	4,712.9
Crops	274.6	4,370.7	1,158.5	5,803.8
Grass	1,683.7	4,313.5	1,474.8	7,472.1
Snow/Ice	6.4	0.0	0.0	6.4
Trees	2,255.6	2,117.2	753.7	5,126.4
Water	494.3	281.5	50.7	826.5
Sum	5,585.8	17,459.9	4,091.8	27,137.4
Panel B: Relative Land Use				
Artificial	9.2%	13.7%	6.8%	11.8%
Bare	6.4%	22.8%	9.2%	17.4%
Crops	4.9%	25.0%	28.3%	21.4%
Grass	30.1%	24.7%	36.0%	27.5%
Snow/Ice	0.1%	0.0%	0.0%	0.0%
Trees	40.4%	12.1%	18.4%	18.9%
Water	8.8%	1.6%	1.2%	3.0%
Sum	100.0%	100.0%	100.0%	100.0%

This table illustrates the land use of RE plant units, both separately for individual technologies and in total. The percentages indicate the proportion of the total area occupied by all RE plant units—or those utilizing specific technologies—that is classified as a particular land type. Percentages are calculated based on the total land use of all RE plant units in the sample. Variable definitions can be found in Appendix A.

Table IA.A.2: $STAR_T$ Values and Species-based Biodiversity Measures

	Log($STAR_T$)			
	(1)	(2)	(3)	(4)
Log(#Species (All))	2.66***			
	(42.5)			
Log(#Species (Threatened))		1.82***		
		(60.9)		
Log(Species Threat Score)			0.97***	
			(183)	
$STAR_R$				0.67***
				(108)
Observations	44,441	44,192	44,439	43,780
Adj. R^2	0.10	0.15	0.56	0.41

This table relates the $STAR_T$ scores of RE plants to species-based measures of biodiversity impact. #Species (All) and #Species (Threatened) measure the number of all species, or those that are threatened, by a RE plant. Species Threat Score is a threat-weighted species-overlap score. $STAR_R$ is the potential impact that habitat restoration in an area can have on reducing global species extinction risks. Regressions are conducted at the plant-unit level. *t*-statistics based on robust standard errors clustered by power plants are presented in parentheses. ***, ** and * indicate significance at the 1%-, 5%- and 10%-levels, respectively. Variable definitions can be found in Appendix A.

Table IA.A.3: Aggregate Quantification of Biodiversity Impacts in Top-30 Countries

	$STAR_T$ (in million)				Capacity
Country	Total	Hydro	Solar	Wind	(in GW)
USA	708.20	10.62	657.00	40.60	318.81
India	581.80	398.60	165.10	18.06	99.15
China	521.90	324.10	163.50	34.32	437.42
Vietnam	363.40	353.30	6.56	3.58	25.87
Mexico	338.90	123.80	191.60	23.57	21.21
Sri Lanka	277.40	273.10	0.07	4.24	1.00
Brazil	225.20	164.40	26.02	34.84	93.51
Colombia	169.40	165.50	3.92	0.03	5.94
Japan	153.90	5.12	133.00	15.79	22.34
Australia	139.40	3.87	123.10	12.38	25.85
Laos	128.50	120.70	0.00	7.79	10.03
Spain	117.00	5.82	92.35	18.84	48.44
Ecuador	98.34	90.92	6.12	1.31	3.68
Costa Rica	96.59	75.78	0.19	20.61	1.56
Malaysia	89.92	82.34	7.58	0.00	5.40
Philippines	88.41	23.93	23.86	40.62	6.18
Cambodia	78.28	77.62	0.66	0.00	1.84
Reunion	77.23	1.05	75.42	0.76	0.11
Indonesia	54.87	49.26	5.60	0.00	3.30
Peru	48.32	37.95	1.76	8.61	5.08
Iran	37.74	37.60	0.11	0.02	11.24
Chile	34.01	11.95	16.46	5.60	16.40
Mauritius	32.73	0.00	31.42	1.31	0.09
Turkey	31.02	24.27	1.96	4.80	33.68
Myanmar	30.42	30.42	0.00	0.00	2.97
Israel	27.23	0.15	26.97	0.10	2.54
Dominican Republic	26.89	15.62	8.58	2.68	1.05
South Africa	25.64	11.62	8.86	5.16	10.04
Hungary	24.59	0.00	24.58	0.01	1.20
New Zealand	23.77	19.11	0.00	4.66	1.43
Sum	4,651	2,539	1,802	310	1,217

This table lists the 30 countries with the highest aggregate $STAR_T$ score. Next to the aggregate $STAR_T$ scores (in million), we also report the capacity (in GW) of RE plants in a country.

Table IA.A.4: Plant-Level Quantification of Biodiversity Impacts by Plant Technology

	Obs.	Mean	p25	p50	p75	SD
Panel A: Hydro Plants						
$STAR_T$ (thousand)	13,556	197.69	0.30	2.56	24.96	1,493.27
$\frac{STAR_T}{MWh}$	13,556	26.74	0.04	0.22	1.60	403.62
$\frac{STAR_T}{1{,}000m^2}$	13,556	1,292.43	11.02	72.34	349.63	5,757.24
Area (km^2)	13,556	0.41	0.01	0.04	0.17	1.65
Capacity (MW)	13,556	45.16	2.75	7.85	30.20	107.85
Generation (GWh)	13,556	150.34	9.15	26.13	100.53	359.03
Panel B: Solar Plants						
$STAR_T$ (thousand)	17,715	110.58	0.18	2.60	14.49	1,707.19
$\frac{STAR_T}{MWh}$	17,715	15.52	0.03	0.42	2.20	208.95
$\frac{STAR_T}{1{,}000m^2}$	17,715	105.26	0.46	5.06	20.22	1,188.60
Area (km^2)	17,715	0.99	0.35	0.50	0.69	2.21
Capacity (MW)	17,715	23.43	2.00	5.00	15.00	64.82
Generation (GWh)	17,715	51.31	4.38	10.95	32.85	141.95
Panel C: Wind Plants						
$STAR_T$ (thousand)	16,345	22.18	0.01	0.15	2.49	234.01
$\frac{STAR_T}{MWh}$	16,345	0.99	0.00	0.01	0.07	23.28
$\frac{STAR_T}{1{,}000m^2}$	16,344	102.56	0.32	1.89	10.83	2,062.59
Area (km^2)	16,345	0.25	0.04	0.09	0.28	0.45
Capacity (MW)	16,345	35.46	6.00	14.40	40.00	60.85
Generation (GWh)	16,345	105.61	17.87	42.89	119.14	181.23

This table presents summary statistics at the plant-unit level of the biodiversity impact of RE. We report the $STAR_T$ score, the $STAR_T$ density ($STAR_T/1{,}000m^2$), and the $STAR_T$ intensity ($STAR_T$/kWh). We display the number of observations, mean, 25^{th} percentile, median, 75^{th} percentile, and standard deviation. The table additionally reports information on the plant unit's size, capacity, and expected generation. Variable definitions can be found in Appendix A.

Table IA.A.5: Plant-Level Quantification of Biodiversity Impacts by Continent

Variable	Obs.	Mean	p25	p50	p75	SD
Panel A: RE Plants in Africa						
$STAR_T$ (thousand)	921	221.23	0.60	5.35	53.86	1,794.62
$\frac{STAR_T}{MWh}$	921	64.34	0.02	0.28	2.34	622.41
$\frac{STAR_T}{1{,}000m^2}$	921	614.93	4.81	23.56	125.60	3,073.47
Area (km^2)	921	1.30	0.04	0.38	0.77	3.81
Capacity (MW)	921	53.15	4.40	18.00	66.00	80.29
Generation (GWh)	921	159	12	44	197	253
Panel B: RE Plants in Americas						
$STAR_T$ (thousand)	14,362	128.30	0.55	4.33	20.15	1,765.86
$\frac{STAR_T}{MWh}$	14,362	13.78	0.05	0.52	2.49	309.66
$\frac{STAR_T}{1{,}000m^2}$	14,362	456.10	2.11	10.90	51.00	3,229.61
Area (km^2)	14,362	0.87	0.21	0.50	0.70	1.77
Capacity (MW)	14,362	36.35	2.00	5.00	30.00	73.42
Generation (GWh)	14,362	99.94	4.38	12.05	88.46	208.99
Panel C: RE Plants in Asia/Oceania						
$STAR_T$ (thousand)	14,561	188.50	0.34	3.61	28.79	1,512.19
$\frac{STAR_T}{MWh}$	14,561	24.35	0.03	0.21	1.58	275.23
$\frac{STAR_T}{1{,}000m^2}$	14,561	918.79	5.08	37.48	256.59	5,175.31
Area (km^2)	14,561	0.63	0.03	0.17	0.47	2.09
Capacity (MW)	14,561	51.79	4.00	14.40	49.50	112.80
Generation (GWh)	14,561	157.61	12.05	41.70	144.14	350.61
Panel D: RE Plants in Europe						
$STAR_T$ (thousand)	17,772	11.83	0.01	0.12	0.88	305.84
$\frac{STAR_T}{MWh}$	17,772	2.35	0.00	0.01	0.13	92.70
$\frac{STAR_T}{1{,}000m^2}$	17,771	31.83	0.27	1.62	8.58	393.87
Area (km^2)	17,772	0.24	0.03	0.10	0.31	0.60
Capacity (MW)	17,772	15.85	2.95	7.00	16.00	30.77
Generation (GWh)	17,772	44.82	7.88	19.16	45.84	87.50

This table presents summary statistics at the plant-unit level of the biodiversity impact of RE. We report the $STAR_T$ score, the $STAR_T$ intensity ($STAR_T$/MWh), and the $STAR_T$ density ($STAR_T$/1,000m^2). We display the number of observations, mean, 25^{th} percentile, median, 75^{th} percentile, and standard deviation. The table additionally reports information on the plant unit's size, capacity, and expected generation. Variable definitions can be found in Appendix A.

Table IA.A.6: Top-10 Biodiversity Impact States around the World

State	Country	$STAR_T$ (million)	Capacity	Highest Impact Plant in State	
				Name	Technology
California	USA	268.2	31,089.2	Sandrini Solar 2 Project	Solar
Mahārāshtra	India	190.1	4,550.5	Konal Hydro Plant	Hydro
Central Province	Sri Lanka	154.1	373.2	Upper Kotmale Plant	Hydro
Ningxia Ningxia Hui	China	134.8	8,889.5	Tengger Desert Plant	Solar
Puebla	Mexico	129.6	816.5	Pachamama II Solar	solar
Nayarit	Mexico	121.3	1,528.8	El Cajon	Hydro
Sichuan Province	China	119.5	96,924.7	Daqiao Reservoir Plant	Hydro
Guam	USA	116.3	85.7	Mangilao Solar Plant	Solar
New South Wales	Australia	110.7	7,620.8	Metz Solar Plant	Solar
Lam Đong	Vietnam	95.0	947.8	Dong Nai Four Plant	Hydro

This table shows the ten states with the highest cumulative $STAR_T$ scores from RE power plants. States are based on Administrative Level 1 boundaries (i.e., the largest subnational division of a country, such as states in the U.S.). We sort the states based on the $STAR_T$ score. Year is the year in which commercial operation started and capacity is measured in MW. Variable definitions can be found in Appendix A.

Table IA.A.7: Individual Threatened Species Most Affected by RE Plants

Binomial Nomenclature	English Name	Status	Habitat km^2	Habitat %
Panel A: Threatened Species				
Otus feae	Annobon Scops Owl	CR	0.55	3.73%
Thalasseus bernsteini	Chinese Crested Tern	CR	1.17	2.01%
Aerodramus bartschi	Mariana Swiftlet	VU	14.99	1.77%
Pristimantis pulchridormientes	Sleeping Beauty Rain Frog	EN	0.93	1.52%
Pteropus mariannus	Mariana Flying Fox	EN	13.91	1.37%
Ammospermophilus nelsoni	Nelson's Antelope Squirrel	EN	214.53	1.31%
Neurergus microspilotus	Kurdistan Newt	CR	5.13	1.30%
Dipodomys nitratoides	Fresno Kangaroo Rat	VU	144.32	1.27%
Nyctimantis galeata	Brown-eyed Treefrogs	EN	2.80	1.20%
Dipodomys ingens	Giant Kangaroo Rat	EN	77.60	1.14%
Panel B: Critically-Endangered Species				
Otus feae	Annobon Scops Owl	CR	0.55	3.73%
Thalasseus bernsteini	Chinese Crested Tern	CR	1.17	2.01%
Neurergus microspilotus	Kurdistan Newt	CR	5.13	1.30%
Gymnogyps californianus	California Condor	CR	654.96	0.64%
Anaxyrus houstonensis	Houston Toad	CR	74.47	0.37%
Lophura edwardsi	Edward's Pheasant	CR	27.78	0.34%
Aneides caryaensis	HNG Green Salamander	CR	6.13	0.32%
Hynobius amakusaensis	Amakusa Salamander	CR	0.62	0.27%
Pygathrix nemaeus	Dove Langur	CR	232.73	0.25%
Pygathrix cinerea	Gray-shanked Douc	CR	59.22	0.24%

This table shows the species for which most of their habitiat is affected by RE plant units. Panel A includes species that are classified as threatened (vulnerable, endangered, critically endangered) by the IUCN. Panel B only includes species that are classified as critically endangered by the IUCN. The first column shows the species name in bionmial nomenclature, the second column shows the english name, and the third column the extinction risk status according to the IUCN Red List. The fourth column shows the habitat area in square kilometers that overlaps with the land use of the renewable power plants in our sample. The last column shows the affected habitat area scaled by the whole habitat of the species. VU stands for vulnerable, EN for endangered, CR for critically endangered, and HNG for Hickory Nut Gorge.

IA.B. Comparison of STAR Metric to Other Measures

IA.B.1 Overview and Goal

In this Internet Appendix, we compare the STAR metric with several other biodiversity metrics. We use two case studies to illustrate the different measurements and their limitations in our setting. The two case studies, a solar plant located in a desert region in Section IA.B.2 and a solar plant in a tropic region in Section IA.B.3, are selected to highlight the measurements in two very different biodiversity settings. We also present a summary of the different alternative metrics and their limitations in Table IA.B.1.

To ensure a comprehensive evaluation, our selection of metrics aligns with three direct biodiversity measurement categories from the EU Business & Biodiversity Platform (Lammerant et al., 2022). We contrast species-based metrics (STAR, Species Richness) against widely used extent × condition metrics (MSA and Species Loss Characterization Factors) and extent × condition × significance metrics (BII and Marginal Value of Persistence), thereby covering the primary types of measurement approaches available for plant-level estimation.

IA.B.2 Case Study 1: Solar PV Plant in China

IA.B.2.1 Description of Case Study

This case presents and calculates different biodiversity metrics for the Guazhou Solar Power Plant (100 MW) in Guazhou, China, a desert region in Gansu Province. The satellite imagery below shows the plant and surrounding landscape. The plant started in 2015.



IA.B.2.2 STAR Metric

Score: Combining the satellite-derived footprint of 2.48 km^2 with the local STAR$_T$ index values yields a STAR$_T$ score of 4,812 (calculated for the year 2015 in which the plant started).

Assessment: The score accounts for species in this desert ecosystem threatened by the project. Notably, despite the significantly larger land footprint of the Guazhou solar farm compared to the Planta Solar Honda in Section IA.B.3 (2.48 km^2 vs. 0.154 km^2), this plant's biodiversity

impact is about 2.2 times lower (4,812 vs. 10,612). Hence, the STAR metric captures the dramatic difference in local biodiversity richness and extinction risk between a species-poor desert biome and a tropical biodiversity hotspot.

IA.B.2.3 Biodiversity Intactness Index (BII)

Methodology Estimates the average abundance of native species in an area relative to an undisturbed baseline. It combines models of total species abundance with measures of compositional similarity to a pristine reference ecosystem. The resulting intactness metric uses modeled relationships derived from the PREDICTS database, incorporating pressures such as land-use intensity, human population density, and road proximity. A key source for the method is De Palma et al. (2021).

Score: Percentage on a continuous scale from 0% (completely depleted) to 100% (pristine conditions). Since BII data are publicly available only at the country level, the regional average score for China is used. In the case of the plant, the BII score is ∼63% for the year 2015 (BII scores are yearly observations).

Assessment: The average score cannot be linked to specific plants because it is aggregated at regional levels (e.g., country or ecoregion), lacking the spatial precision needed for project-specific impact evaluation. Crucially, intactness in a desert biome is not comparable to intactness in a tropical biodiversity hotspot. This is a key limitation because it quantifies ecosystem degradation relative to a baseline rather than absolute species richness, making cross-biome comparisons problematic (a species-poor desert can score 100% if undisturbed, while a degraded but species-rich tropical forest might score lower). Furthermore, as a pre-packaged model dependent on simulated time-panels rather than dynamic ground-based observations, BII does not offer the flexibility to combine biodiversity indices with specific land-use data. Finally, BII scores lack additivity and cannot be meaningfully aggregated across projects.

IA.B.2.4 Mean Species Abundance (MSA)

Methodology: Expresses the mean abundance of original species in a disturbed area as a proportion of their abundance in an undisturbed reference habitat. The calculation incorporates six pressures: land-use change, infrastructure development, habitat fragmentation, human encroachment, nitrogen deposition, and climate change. The framework covers six major taxonomic groups, including mammals, birds, and plants. The metric is model-based, relying on established pressure-impact relationships from the GLOBIO framework.
Score: Percentage on a scale from 0% (completely destroyed) to 100% (fully intact). In the case of the plant, the regional average derived from global pressure models (GLOBIO) is about ∼82.6% in 2015.

Assessment: The method provides a more detailed, district-level assessment compared to BII, assigning a high score (∼82.6%) to the Guazhou plant to indicate that the desert is relatively "untouched." However, this is potentially misleading because a high percentage of intactness in a species-poor area does not equate to high biodiversity value. This reflects the metrics' fundamental limitation: it indicates "how much is left" but does not quantify absolute species

richness or extinction risk ("what is there"). Hence, the metric suffers from spatial incomparability, as high scores simply indicate an area is undisturbed regardless of its underlying ecological value. The metric fails to reflect the real impact of local infrastructure projects because it is model-based, relying on established pressure-impact relationships rather than direct species impacts.

IA.B.2.5 Species Richness

Methodology: Estimates biodiversity by counting the number of species present within a standardized grid cell, including counts of threatened species and species with small geographic ranges. The calculation involves overlaying species range maps onto a global 10×10 km grid. Data inputs include breeding ranges for birds and IUCN Red List range maps for mammals and amphibians. A key source for the method is (Jenkins, Pimm, and Joppa, 2013).

Score: Count of the number of species present within an area. In the case of the plant, approximately ∼133 species, estimated by calculating the spatial intersection between the Guazhou plant's land-use footprint and IUCN Red List area-of-habitat maps for mammals, amphibians, and birds.

Assessment: The low count accurately reflects the relatively low biodiversity richness of the desert biome. However, the metric treats all species equally; for example, a common lizard counts the same as a critically endangered bird. This fails to distinguish material extinction risk or to capture the relative urgency of conservation action. Additionally, the method acts as a coarse filter, using broad range maps rather than Area of Habitat maps, which means species may be counted as present even if their actual habitat within a grid cell has been destroyed. Finally, the metric provides no insight into the specific ratio/area of habitat impacted by renewable energy plants.

IA.B.2.6 Species Loss Characterization Factors

Methodology: Uses a Countryside Species-Area Relationship (c-SAR) model to predict the number of global species extinctions attributable to different land-use types. The method derives a single Characterization Factor (CF) for each land-use category across 804 terrestrial ecoregions worldwide (rather than at the grid cell level). CFs are weighted using a Vulnerability Score (VS) calculated as the ratio of threatened endemic species richness to total species richness within each ecoregion. A key source for the method is Chaudhary et al. (2015).

Score: Fractional loss of species relative to a baseline, scaled by area and time. In the case of the plant, the score ranges between 1.5×10^{-15} and 6.4×10^{-16}, calculated as the ratio of the global species pool lost per m^2, depending on the land-use type and based on the ecoregion average for the Taklimakan Desert (the closest ecoregion to Guazhou).

Assessment: This approach applies a generic coefficient to an entire ecoregion, assuming that the biodiversity value of the project location is identical to the rest of the Taklimakan Desert. This introduces substantial measurement error. Guazhou is situated in an oasis ecosystem at the edge of the Gobi Desert, featuring a desert-oasis ecotone with distinct vegetation communities, agricultural lands, and water resources. In contrast, the Taklimakan is a hyper-arid

shifting-sand desert where approximately 85% of the land consists of mobile, unstabilized dunes devoid of vegetation. This highlights the metric's primary limitation of coarse spatial resolution, where biodiversity impacts are averaged across entire ecoregions, ignoring site-level variation in habitat quality. Furthermore, the methodology was developed for Life Cycle Assessment (LCA) product-footprinting objectives rather than site-specific conservation targeting, making it less suited for evaluating individual infrastructure projects at precise locations.

IA.B.2.7 Marginal Value of Persistence

Methodology: Quantifies how land conversion affects the probability of local species persistence. It employs a non-linear power law relationship ($P = E^z$) to estimate a persistence score based on remaining habitat area, then distributes the marginal change in persistence (ΔP) across converted land cells. Required inputs include high-resolution Area of Habitat (AOH) maps and historical baseline vegetation data representing pre-anthropogenic conditions. A key source for the method is Durán et al. (2020).

Score: Persistence score (P) between 0 and 1 calculated as $P = E^z$ with E being the proportion of original habitat remaining and z the extinction coefficient (typically 0.25). In the case of the plant, data are not available to evaluate the plant.

Assessment: The metric requires accurate historical baseline maps (e.g., pre-16th-century vegetation) to calculate habitat depletion curves. Such data are not available for many regions, rendering the methodology infeasible in many settings. Beyond this high data requirement, the metric is designed for attribution rather than opportunity identification, focusing on ex-post assignment of responsibility for historical biodiversity loss rather than ex-ante identification of conservation intervention opportunities. Lastly, there is an aggregation problem: the non-linear nature of the persistence function makes simple addition of marginal values across a portfolio of sites mathematically complex and potentially inconsistent for applications that require additive metrics.

IA.B.3 Case Study 2: Solar PV Plant in Colombia

IA.B.3.1 Description of Case Study

This case presents biodiversity metrics for the Planta Solar Honda (10 MW) located in Guaduas, Colombia, a tropical region in the Magdalena Valley of the Andes. The satellite imagery below shows plant and surrounding landscape. The plant started in 2023.



IA.B.3.2 STAR Metric

Score: Combining the satellite-derived footprint of 0.154 km^2 with local STAR$_T$ index values yields a STAR$_T$ score of 10,612 (start of the plant in 2023).

Assessment: Although the land footprint is about 16.1 times smaller than that of the Guazhou project, the total biodiversity impact is about 2.2 times higher. This demonstrates the metric's sensitivity to local ecological conditions, accurately reflecting the high biodiversity density and extinction risk inherent to the tropical Andes.

IA.B.3.3 Biodiversity Intactness Index (BII)

Score: Percentage on a continuous scale from 0% (completely depleted) to 100% (pristine conditions). In the case of the plant, using the country-level aggregate for Colombia, the regional average score is ∼72% in 2023.

Assessment: The metric fails to reflect the massive difference in absolute biological richness between Guazhou and Guaduas. While it suggests declining intactness over time, it misses the critical point that destroying one hectare here is far more damaging to global biodiversity than one hectare in a desert biome. This highlights a primary limitation: the metric measures ecosystem degradation relative to a baseline rather than absolute species richness; consequently, a species-poor desert can score 100% if undisturbed, while a degraded but species-rich tropical forest might score lower, making cross-biome comparisons problematic. Additionally, the "time-panel" is simulated based on changes in pressure inputs rather than dynamic ground-based observations, and the data are typically aggregated at regional levels (e.g., country or ecoregion), lacking the spatial precision needed for project-specific biodiversity-impact evaluation. Finally, as a pre-packaged model, it does not offer the flexibility to combine biodiversity indices with specific land-use data, and as with the Guazhou case, the metric lacks additivity and cannot be meaningfully aggregated across projects.

IA.B.3.4 Mean Species Abundance (MSA)

Score: Percentage on a scale from 0% (completely destroyed) to 100% (fully intact). In the case of the plant, the regional average derived from GLOBIO models is approximately ∼57.0% in 2023.

Assessment: MSA assigns a low score (∼57.0%), correctly reflecting habitat degradation, but paradoxically makes Guaduas appear "less valuable" than Guazhou (57.0% vs. 82.6%). In reality, the per-area STAR density in Guaduas is about 35 times higher than in Guazhou. This highlights a key limitation: MSA is a relative intactness measure indicating the proportion of original biodiversity remaining ("how much is left") rather than quantifying absolute species richness or extinction risk ("what is there"). Consequently, it suffers from spatial incomparability, where scores reflect disturbance levels rather than ecological value—for example, an intact desert and an intact tropical rainforest would both score highly despite vastly different species richness. Furthermore, the metric is model-based, relying on established pressure-impact relationships from the GLOBIO framework rather than direct species surveys. As a result, MSA fails to capture material biodiversity risk differences and cannot be meaningfully aggregated across assets.

IA.B.3.5 Species Richness

Score: Count of the number of species present within an area. In the case of the plant, about ∼504 species, estimated through spatial intersection with IUCN Red List habitat maps.

Assessment: The high count accurately reflects the tropical diversity of the Magdalena Valley, but the metric treats all species equally regardless of their conservation status. Without risk-weighting, it fails to quantify the urgency of conservation in this valley. This highlights the method's primary limitations: it acts as a coarse filter, using broad range maps rather than Area of Habitat (AOH) maps, which means species may be counted as present in a grid cell even if their actual habitat within that cell has been destroyed. Furthermore, by treating all threatened species equally regardless of their extinction risk level, it fails to capture the relative urgency of conservation action. Finally, the metric provides no insight into the specific ratio/area of habitat impacted by renewable energy plants.

IA.B.3.6 Species Loss Characterization Factors

Score: Fractional loss of species relative to a baseline, scaled by area and time. In the case of the plant, the score ranges from 6.23×10^{-14} to 3.41×10^{-13}, calculated as the ratio of the global species pool per m^2, depending on the land-use type and based on the ecoregion average for the Magdalena Valley montane forests.

Assessment: The approach assumes homogeneous biodiversity impact across the valley and cannot provide precise asset-level estimates. It ignores local habitat heterogeneity and the specific footprint of the solar plant, which spans dry forest fragments, agricultural land, and riparian corridors along the Magdalena River.

Assessment: This approach assumes homogeneous biodiversity impact across the valley and cannot provide precise asset-level estimates. It ignores local habitat heterogeneity and the

specific footprint of the solar plant, which spans dry forest fragments, agricultural land, and riparian corridors along the Magdalena River. This illustrates the metric's key limitation: coarse spatial resolution, where biodiversity impacts are averaged across entire ecoregions, assuming homogeneity within large geographic areas. Additionally, the methodology was developed for Life Cycle Assessment (LCA) applications, where the goal is to estimate the biodiversity footprint embedded in products (e.g., comparing bioethanol feedstocks). This product-footprinting objective differs fundamentally from site-specific conservation targeting, where the aim is to evaluate the biodiversity impact of individual infrastructure projects at precise locations.

IA.B.3.7 Marginal Value of Persistence

Score: Persistence score (P) between 0 and 1 calculated as $P = E^z$ with E being the proportion of original habitat remaining and z the extinction coefficient (typically 0.25). In this case, data are not available to assess the plant.

Assessment: The methodology relies on historical baseline vegetation maps to estimate habitat depletion curves. Such baselines are only available for select regions, rendering the metric unsuitable for global, asset-level biodiversity analysis. Beyond this high data requirement, the metric is designed for attribution rather than opportunity identification, focusing on ex-post assignment of responsibility for historical biodiversity loss rather than ex-ante identification of conservation intervention opportunities. Lastly, there is an aggregation problem: the non-linear nature of the persistence function makes simple addition of marginal values across a portfolio of sites mathematically complex and potentially inconsistent for applications that require additive metrics.

Table IA.B.1: Alternative Biodiversity Metrics

Metric	Methodology	Score	Limitations	Applications
Biodiversity Intactness Index (BII)	Estimates the average abundance of native species in a given area relative to an undisturbed baseline. The metric uses modeled relationships derived from the PREDICTS database, incorporating pressures such as land use intensity, human population density, and road proximity.	Percentage on a continuous scale ranging from 0% (completely depleted) to 100% (pristine conditions).	• Measures ecosystem degradation relative to a baseline rather than absolute species richness; consequently, a species-poor desert can score 100% if undisturbed, while a degraded but species-rich tropical forest might score lower, making cross-biome comparisons problematic. • Is "time-panel" simulated based on changes in pressure inputs rather than dynamic ground-based observations. • Is typically aggregated at regional levels (e.g., country or ecoregion), lacking the spatial precision needed for project-specific biodiversity-impact evaluation. • metric is based on a pre-packaged model and does not offer the flexibility to combine biodiversity indices with specific land-use data.	Schneider et al. (2024) utilize the BII to model trade-offs in future land-use scenarios, projecting that a profit-driven global cropland expansion of 3.6% by 2030 would result in a 26% decline in biodiversity intactness within the newly expanded areas.
Mean Species Abundance (MSA)	Expresses the mean abundance of original species in a disturbed area as a proportion of their abundance in an undisturbed reference habitat. The calculation incorporates six pressures: land use change, infrastructure development, habitat fragmentation, human encroachment, nitrogen deposition, and climate change. The framework covers six major taxonomic groups, including mammals, birds, and plants. Builds on the GLOBIO model.	Percentage on a scale from 0% (completely destroyed) to 100% (fully intact).	• Is a relative intactness measure, which indicates the proportion of original biodiversity remaining ("how much is left") rather than quantifying absolute species richness or extinction risk ("what is there"). • Suffers from spatial incomparability: high scores simply indicate that an area is relatively undisturbed but provide no information about the underlying ecological value. For example, an intact desert and an intact tropical rainforest would both score highly despite vastly different species richness. • Is model-based, relying on established pressure-impact relationships from the GLOBIO framework rather than direct species surveys.	Schipper et al. (2020) apply MSA to project global biodiversity trends under Shared Socioeconomic Pathways (SSPs), finding that land-use change remains the dominant driver of terrestrial biodiversity loss through 2050.
Species Richness	Estimates biodiversity by counting the number of species present within a standardized grid cell, including counts of threatened species and species with small geographic ranges. The calculation involves overlaying species range maps onto a global 10×10 km grid (using an equal-area projection). Data inputs include breeding ranges for birds and IUCN Red List range maps for mammals and amphibians.	Count of the number of species present within an area.	• Acts as a coarse filter, using broad range maps rather than Area of Habitat (AOH) maps that account for suitable habitat within a species' range. This means species may be counted as present in a grid cell even if their actual habitat within that cell has been destroyed. • Has no risk weighting, treating all threatened species equally regardless of their extinction risk level and failing to capture the relative urgency of conservation action. • Faces an action gap: while species richness maps identify where species occur, they do not indicate what interventions would most effectively reduce extinction risk (e.g., threat abatement vs. habitat restoration).	Montesino Pouzols et al. (2014) integrate distribution data for 24,757 terrestrial vertebrate species into a spatial prioritization framework for global protected area expansion.

Continued on next page...

Table IA.B.1 continued

Metric	Methodology	Score	Limitations	Applications)
Species Loss Characterization Factors	Uses a Countryside Species-Area Relationship (c-SAR) model to predict the number of global species extinctions attributable to different land use types. The method derives a single Characterization Factor (CF) for each land use category across 804 terrestrial ecoregions worldwide (rather than at the grid cell level). CFs are weighted using a Vulnerability Score (VS) calculated as the ratio of threatened endemic species richness to total species richness within each ecoregion.	Fractional loss of species relative to a baseline, scaled by area and time.	• Has a coarse spatial resolution: biodiversity impacts are averaged across entire ecoregions, assuming homogeneity within large geographic areas and ignoring site-level variation in habitat quality and species distributions. • Is designed to predict future species loss resulting from land use change, rather than to quantify current opportunities for reducing extinction risk. • Was developed for Life Cycle Assessment (LCA) applications, where the goal is to estimate the biodiversity footprint embedded in products (e.g., comparing bioethanol from different feedstocks). This product-footprinting objective differs fundamentally from site-specific conservation targeting, where the aim is to evaluate and compare the biodiversity impact of individual infrastructure projects at precise locations.	Chaudhary et al. (2015) apply characterization factors to compare land use biodiversity impacts of bioethanol production from six different feedstocks across world regions.
Marginal Value of Persistence	Quantifies how land conversion affects the probability of local species persistence. It employs a non-linear power law relationship ($P = E^z$) to estimate a persistence score based on remaining habitat area, then distributes the marginal change in persistence (ΔP) across converted land cells. Required inputs include high-resolution Area of Habitat (AOH) maps and historical baseline vegetation data representing pre-anthropogenic conditions.	Persistence score (P) between 0 and 1 calculated as $P = E^z$ with E being the proportion of original habitat remaining and z the extinction coefficient (typically 0.25).	• Has a high data requirement, requiring accurate historical baseline data (e.g., pre-16th century vegetation maps) that are often unavailable or unreliable at global scales. • Is designed for attribution rather than opportunity identification, focusing on ex-post assignment of responsibility for historical biodiversity loss rather than ex-ante identification of conservation intervention opportunities. • Brings an aggregation problem: the non-linear nature of the persistence function makes simple addition of marginal values across a portfolio of sites mathematically complex and potentially inconsistent for applications that require additive metrics.	Durán et al. (2020) apply the marginal value framework to the Brazilian Cerrado to assess biodiversity impacts of land conversion on over 2,000 species of amphibians, birds, mammals, and plants between 2000 and 2014.

This table compares various potential alternatives to the STAR metric. It explains the respective methodologies (definition, calculation, inputs) and provides assessments regarding each method's limitations for site-specific measurements of biodiversity impacts. These assessments highlight why our approach employs the STAR metric. We also provide examples of research where the other metrics are used. The selection of metrics aligns with the biodiversity measurement categories by the EU Business & Biodiversity Platform (Lammerant et al., 2022).

IA.C. Details about STAR Estimation for Small Solar Plants

For solar plants below 10 MW capacity, we rely on an indirect estimation method rather than direct satellite-image delineation. These plants are often too small, fragmented, or embedded within built environments for reliable land-use footprint detection from medium-resolution satellite imagery. Applying the direct solar-farm detection algorithm to such plants would generate a substantial amount of false positives and false negatives. We therefore estimate their land-use footprint indirectly.

For each small solar unit i, we estimate its land use using a log-linear regression model that is trained on solar plants with more than 10 MW for which we have directly measured footprints:

$$\log(A_i) = \alpha + \beta_1 \text{Capacity}_i + \beta_2 \text{Year}_i + \varepsilon_i,$$

where A_i is the plant's land-use footprint in m^2, Capacity_i is its nameplate capacity in MW, and Year_i is its start year of commercial operation.

We then assign the local STAR_T values and land type using a point-buffer calculation around the plant's coordinates from the S&P database using a 2.5 km buffer in Google Earth Engine. Within this buffer, we calculate the mean STAR_T value per m^2 and the local land-cover shares using the GLC-FCS30D land-cover layer, reclassified into seven categories: artificial, bare, crops, grass, snow/ice, trees, and water.

The plant-level STAR_T score is then calculated as:

$$\text{STAR}_{T,i} = \overline{\text{STAR}}_{T,i}^{2.5\text{km}} \times A_i \times (1 - \text{LandBuilt}_i),$$

where $\overline{\text{STAR}}_{T,i}^{2.5\text{km}}$ is the mean STAR_T intensity in the 2.5 km buffer and LandBuilt_i is the built-up land share in the same buffer. The built-up-land adjustment prevents assigning biodiversity loss to land that is already built up (having little to none biodiversity value).

Small solar units located on urban rooftops, as well as units located on artificial land such as reclaimed land or engineered islands, are retained in the plant universe but assigned zero biodiversity impact. We discuss the identification and treatment of built-up and artificial-land plants in detail below. For units with unusable coordinates or locations on open water, STAR values are left missing because biodiversity impact cannot be calculated reliably.

IA.D. Details about STAR Estimation for Fossil/Nuclear Plants

For fossil-fuel and nuclear plants, we use an indirect estimation method because their land-use footprints cannot be identified consistently with the same satellite-imagery approach used for large solar farms or hydropower reservoirs. Thermal power plants typically have a much smaller spatial extent than utility-scale solar farms or hydropower reservoirs, and they contain heterogeneous components, including generation blocks, storage yards, cooling systems, service roads, and auxiliary buildings. These components do not have a uniform spectral signature, and automated global footprint detection would therefore introduce substantial measurement error. We instead estimate land use from a manually delineated training sample and apply the resulting model to the full fossil/nuclear sample.

$$\log(A_i) = \alpha_g + \beta_{1g}\text{Capacity}_i + \beta_{2g}\text{Year}_i + \varepsilon_i,$$

where A_i is the plant footprint in m^2, Capacity_i is a unit's nameplate capacity in MW, Year_i is the start year of commercial operation, and $g \in \{1\text{–}10, 10\text{–}100, 100\text{–}1000, 1000+\}$ denotes the unit's capacity group. The models are trained on fossil and nuclear plants for which we manually delineated the physical plant footprint in satellite imagery. In the current data build, this training set contains 353 manually delineated footprint polygons, covering 413 plant sites and 1,449 plant-unit observations. When multiple units share the same plant site, the measured footprint is allocated across units in proportion to unit capacity.

We then assign STAR intensity and land-cover composition using a point-buffer calculation around the plant coordinate. In the final data build, fossil and nuclear units are scored using a 2.5 km geodesic buffer in Google Earth Engine. Within this buffer, we calculate the mean STAR Threat Abatement score per m^2 and the local land-cover shares using the GLC-FCS30D land-cover layer, reclassified into seven categories: bare, built, crops, grass, snow/ice, trees, and water.

The plant-level STAR_T score is then calculated as:

$$\text{STAR}_{T,i} = \overline{\text{STAR}}_{T,i}^{2.5\text{km}} \times A_i \times (1 - \text{LandBuilt}_i),$$

where $\overline{\text{STAR}}_{T,i}^{2.5\text{km}}$ is the mean STAR_T intensity in the 2.5 km buffer and LandBuilt_i is the built-up land share in the same buffer. The built-up-land adjustment prevents assigning biodiversity loss to land that is already built and has little or no biodiversity value.

Fossil and nuclear units located on artificial land, such as reclaimed land or engineered islands, are retained in the plant universe but assigned zero biodiversity impact. We discuss the identification and treatment of built-up and artificial-land plants in detail below. For units with unusable coordinates, STAR values are left missing because biodiversity impact cannot be calculated reliably.

IA.E. Details about STAR Estimation for Planned Power Plants

To calculate the biodiversity impact of planned power plants, we again use the STAR_T score. In contrast to existing plants, we cannot use satellite imagery to delineate plant footprints, because the plants are not yet finished. We therefore estimate the biodiversity impact indirectly, using a plant's reported capacity, fuel type, and expected year of commercial operation together with remote-sensing information about the area surrounding its planned location. To calculate the STAR_T score for planned power plants, we proceed in three steps.

Step 1: Indirect Area Measurement

For **solar** and **hydro** (water) plants, we fit a log-linear specification of the form $\log(\text{Area}) = \alpha + \beta_1 \log(\text{Capacity}) + \beta_2 \,\text{Year} + \varepsilon$, on the existing-plant sample for which area is directly measured. The motivation is that capacity is the dominant determinant of plant area, and the year of commercial operation captures efficiency gains that reduce the area required per unit of capacity over time. For fossil-fuel and nuclear plants, we estimate the same model separately within four capacity bins (1–10, 10–100, 100–1,000, and above 1,000 MW), because the area–capacity relationship is markedly non-linear across these scales. For wind plants, we use the same land-cover-weighted area formula as in our main wind analysis. Predicted area is the product of the number of turbines and a land-cover-weighted per-turbine benchmark, where the turbine count is obtained by dividing the plant's capacity by the rated capacity of its reported turbine model, and the per-turbine benchmark adjusts a fixed turbine-pad area for the share of trees, grass, cropland, and bare land in the plant's surroundings. For planned wind units that do not have a reported turbine model, we apply a capacity-based version of the same formula in which the per-MW benchmark replaces the per-turbine benchmark.

Step 2: STAR_T per m^2 around Plant Location

For each planned plant we draw a 2.5 km geodesic buffer around its reported coordinates and compute the spatial average of STAR_T/m^2 within that buffer. From the same buffer we also compute the fractional composition of the seven land types used in the analysis. The 2.5 km radius matches the buffer used to score every other indirect-estimation cohort in the paper.

Step 3: STAR_T per Planned Plant

The total STAR_T score for each planned plant is the product of its predicted area, the average STAR_T/m^2 in its buffer, and the share of natural land in that buffer:

$$\text{STAR}_{T,p} \;=\; s_p \cdot A_p \cdot (1 - L_p),$$

where s_p is the buffer-average STAR_T/m^2, A_p is the predicted area from Step 1, and L_p is the artificial-land share of the buffer. The $(1 - L_p)$ factor down-weights any portion of the planned site that is expected to be built on already-developed land, on which the biodiversity value is approximately zero.

In addition to this multiplicative discount, two categories of planned units receive special treatment by construction. Rooftop solar units are assigned a STAR_T score of zero, because they are mounted on already-built infrastructure with negligible biodiversity value. These units remain in the planned dataset and contribute to capacity totals, but their biodiversity

impact is recorded as zero. Offshore planned units (offshore wind and floating photovoltaic, whose reported coordinates are located on water) and planned units with missing or incorrect coordinates are excluded from the biodiversity calculation entirely: their STAR_T, area, and land-type fields are left as missing (NaN). For offshore units this reflects that the STAR_T framework is land-based and does not apply at their location; for units with invalid coordinates it reflects that the calculation cannot be evaluated. These units are still retained in the planned dataset for capacity-side analyses.

IA.F. Details about Artificial Land Identification

This section explains how we deal with power plants that are built on artificial land. This is important because artificial land has already been altered from its natural state and thus has usually very low biodiversity value. Thus, attributing a STAR-based biodiversity loss to the plant's land-use footprint would overstate the biodiversity harm caused by the plant. We therefore identify plants that are built on artificial land and then set their STAR_T score to zero. As artificial land, we consider pre-built areas such as human settlements (with rooftop solar plants as special case) and reclaimed land.

IA.F.1 Human Settlements

For power plants that overlap with human settlements but are not classified as rooftop solar plants, we classify this overlapping area as artificial land. This distinction is important because many ground-mounted plants contain a mixture of land-cover types: part of the footprint may overlap with roads, buildings, substations, paved surfaces, or other pre-existing built-up land, while the rest may still occupy natural or semi-natural land. plant's biodiversity impact to zero merely because some portion of its footprint is classified as artificial land.

To identify the artificial-land share of each plant footprint, we use the built-up class in the LCLUC2000 land-cover layer. For directly measured plants, we calculate the share of built-up land within the mapped plant footprint. For indirectly measured plants, we use the same spatial support as in the plant-level STAR calculation and calculate the built-up share within that support. We denote this share by L_p, where $L_p \in [0, 1]$ is the fraction of the plant footprint classified as artificial land. The STAR_T score is then calculated only on the non-artificial share of the footprint. Specifically, if A_p is the plant's land-use area and s_p is the local STAR_T/m^2 value, the plant's biodiversity impact is calculated as

$$\text{STAR}_p = s_p \times A_p \times (1 - L_p).$$

Thus, artificial land inside the footprint is excluded from the biodiversity-impact calculation, while the remaining natural-land share is still counted. This approach avoids overstating biodiversity loss for plants that partly occupy pre-existing built environments, but it does not remove the biodiversity impact of the natural or semi-natural land that is actually converted by the plant. Rooftop solar plants are treated separately in Section IA.F.2. Unlike ordinary ground-mounted plants with some artificial land in their footprint, rooftop PV systems are built on top of pre-existing buildings and are therefore assigned a STAR_T score of zero.

IA.F.2 Rooftop Solar Plants

A subset of small solar power plants in the S&P MI database are commercial rooftop photovoltaic (PV) systems mounted on the roofs of buildings in dense urban areas—typically large office complexes, warehouses, residential blocks, and similar built environments. Because rooftop PV sits on top of pre-existing built infrastructure, it does not displace natural habitat. Attributing a STAR-based biodiversity loss to such plants would overstate the harm caused by the generating unit. To identify rooftop PV plants and set their STAR_T score to zero, we proceed in three steps.

Step 1: Urban-Area Flag

Rooftop installations are restricted to small solar plants by construction—utility-scale solar farms cannot be mounted on building roofs. We therefore restrict the rooftop check to solar plants with capacity below 10 MW. For each such plant, we test whether its reported coordinates fall inside the Global Urban Boundaries 2015 layer constructed from the Global Artificial Impervious Area (GAIA) database developed by Li et al. (2020). GAIA maps global urban boundaries and artificial surfaces annually at a 30-meter resolution. Plants whose coordinates intersect an urban polygon are flagged as candidates for being rooftop PV. This initial pass flags 2,045 small solar plants.

Step 2: Manual Review

The urban-area flag is a coarse filter: it can incorrectly classify small utility-scale solar farms that happen to be sited inside or adjacent to a city. We therefore manually inspect each of the 2,045 candidates using high-resolution satellite imagery, and for each plant the reviewer determines whether the reported coordinates correspond to a rooftop PV installation or to a small ground-mounted solar farm. We confirm 1,464 plants as rooftop PV with no significant biodiversity value. The remaining 581 plants are returned to the standard biodiversity-impact calculation.

Step 3: STAR$_T$ Adjustment

For the 1,464 plants confirmed as rooftop PV, we set their STAR$_T$ score to zero. These plants are retained in the dataset and contribute to aggregate capacity, but their biodiversity impact is zero by construction. Importantly, because the S&P MI database focuses on utility-scale plants and we restrict our sample to plants with a capacity of at least 1 MW (due to incomplete coverage of smaller plants), the number of rooftop PV plants in our sample is not representative of their true scale.

IA.F.3 Reclaimed Land

A subset of power plants in the S&P MI database are built on ground that was open water in historical satellite records—landfills, polders, or engineered coastal islands, which we collectively refer to as reclaimed land. If the site had already been converted from its natural state (typically open sea or tidal flats) well before a plant was constructed. To identify power plants on reclaimed land and set their biodiversity impact to zero, we proceed in four steps.

Step 1: Historical Water Coverage

The JRC Global Surface Water (v1.4) Yearly History collection classifies every 30 m pixel on Earth for every year since 1984 as permanent water, seasonal water, or land. We flag every plant whose reported coordinates sit on a pixel that was classified as water in the first year it was observed by JRC and as land in the most recent observation. This initial pass flags 971 plants as candidates for being built on reclaimed land.

Step 2: 10-km Coastal Filter

A water-to-land transition does not have to be human-made. It can also occur far inland—along rivers that have shifted course, oxbow lakes, or floodplains drained for agriculture—where a plant is not on an artificial island but on ground that may retain high biodiversity value. We therefore drop from the candidate set any plant whose coordinates lie more than 10 km from the global ocean boundary. This filter excludes 500 inland candidates and leaves 471 coastal candidates for further review.

Step 3: Manual Check

Even within 10 km of the coast, not every plant flagged by the JRC water-history mark is on reclaimed land. Plants near estuaries, natural deltas, or seasonally inundated mudflats can sit on ground that was legitimately water in early JRC images but is firm, biodiversity-bearing land today—the result of natural sedimentation rather than human reclamation. We manually inspect each of the 471 coastal candidates and confirm 358 of them as built on reclaimed land with no significant biodiversity value. The remaining 113 are released back into the standard biodiversity-impact calculation.

Step 4: STAR$_T$ Adjustment

For the 358 plants confirmed as built on reclaimed land, we set their STAR$_T$ score to zero. The plants are retained in the dataset and contribute to capacity totals, but their biodiversity impact is recorded as zero by construction.

IA.G. Details about Counterfactual Calculation

We calculate counterfactual STAR scores to ask how much the biodiversity impact of a RE plant could be reduced if the same plant had been built at a nearby alternative site, while holding fixed the global STAR_T raster and the plant's physical footprint. We consider four search radii around each plant's current location, $d \in \{10, 20, 50, 100\}$ km. The counterfactual analysis is restricted to operating solar and wind plant units with non-zero actual STAR_T scores. We exclude hydropower plants because feasible hydro locations are tied to river, reservoir, and elevation constraints that are not captured by a generic land-based relocation grid. Rooftop solar units and reclaimed-land/artificial-island units are retained in the data at zero by design and are not part of the counterfactual sample. The final counterfactual sample contains 16,330 solar units and 16,409 wind units. To calculate the counterfactual STAR_T score, we proceed in five steps.

Step 1: Build Test Region

This step defines the geographic universe of possible alternative sites. For every plant location we draw a 100-km geodesic buffer and dissolve the union of all buffers into a single global candidate polygon. We then erase two classes of cells that are not viable siting candidates: mid-ocean areas, using a water-surface mask derived from the JRC Global Surface Water dataset, and urban land, using the Global Urban Boundaries 2015 (GUB) layer. After both erasures, the candidate polygon covers 66.86 million km^2:

Stage	Area (km^2)	% of Raw
Raw dissolved 100-km buffer	84,761,462	100.0 %
After ocean erase	67,476,524	79.6 %
After ocean + urban erase	66,861,595	78.9 %

The 100-km radius is the upper bound of the search; we restrict every counterfactual to land within 100 km of the plant's current location. The 10, 20, and 50 km counterfactuals reuse the same candidate grid: in Step 4 we simply restrict the search to the subset of points that lie within the relevant radius of each plant, so the four candidate sets are nested.

Step 2: Fill the Region with a 1-km Candidate Grid

The allowed polygon is rasterized to a regular 1-km grid in the same equal-area projection, with one candidate point at each cell centre, producing 66,861,619 points. Building a single shared grid over the union of all plant buffers—rather than a separate candidate set inside each plant's own 100-km buffer—avoids the heavy redundancy that arises because plant buffers overlap, scoring each 1-km cell exactly once instead of once per overlapping plant.

Step 3: Score Candidate Locations

Every candidate point and every plant is scored with the same procedure used to compute STAR_T/m^2 in our main analysis. Specifically, we draw a 2.5-km geodesic buffer around the point and take the spatial average of the Threat Abatement score within that buffer. The plant footprint is held fixed throughout: the counterfactual asks what the impact would be if the same

physical plant were built elsewhere, so plant size and capacity do not change. The footprint enters only in Step 4, when STAR_T/m^2 is multiplied by the plant's land-use area to obtain a total counterfactual STAR_T score.

Step 4: Add Buildability Screens

We additionally require that counterfactual sites are buildable land. For this purpose, we add a topographic buildability screen using slope derived from the Copernicus Digital Elevation Model. Following renewable-energy technical-potential screening practices used by the National Renewable Energy Laboratory (NREL), which exclude steep terrain when identifying buildable land for utility-scale projects, candidate points are classified into three slope classes:

$$\begin{aligned} \text{slope class} = 0: &\quad \text{slope} \leq 5\%, \\ \text{slope class} = 1: &\quad 5\% < \text{slope} \leq 20\%, \\ \text{slope class} = 2: &\quad \text{slope} > 20\%. \end{aligned}$$

Counterfactual sites for solar plants are classified as buildable only if slope class $= 0$, while those for wind plants are classified as buildable if slope class $\in \{0, 1\}$. Thus, for a solar plant p, an alternative candidate point q is admissible within radius d only if

$$\text{dist}(p, q) \leq d, \qquad \text{slope}_q \leq 5\%.$$

For a wind plant, the corresponding admissibility rule is

$$\text{dist}(p, q) \leq d, \qquad \text{slope}_q \leq 20\%.$$

Step 5: Counterfactual STAR_T Score per Plant

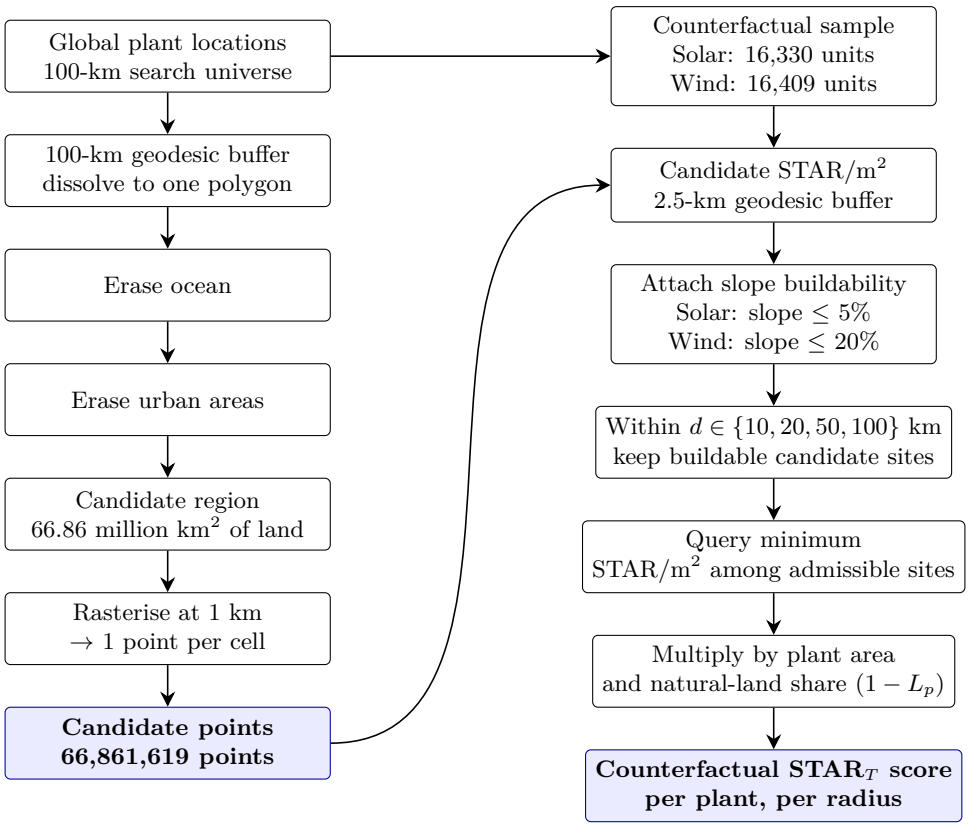
For each plant p and each radius d, we identify all admissible candidate points within distance d of the plant and take the minimum of their STAR_T/m^2 values,

$$s_p^*(d) \;=\; \min_{q \in \mathcal{Q}_p(d)} \; s_q.$$

Here $\mathcal{Q}_p(d)$ denotes the set of candidate points within distance d that satisfy the technology-specific resource and buildability screens described above. This minimum represents the most biodiversity-friendly technically feasible site reachable within the radius. The four radii are nested by construction—the 100-km candidate set contains the 50-km, 20-km, and 10-km sets—so the counterfactual is monotone in d: $s_p^*(100) \leq s_p^*(50) \leq s_p^*(20) \leq s_p^*(10)$ for every plant with admissible candidates at each radius.

The plant-specific counterfactual STAR_T score is obtained by multiplying $s_p^*(d)$ by the plant's land-use area and the natural-land share $(1 - L_p)$, where L_p is the artificial-land fraction of the footprint. The corresponding reduction ratio compares this counterfactual to the plant's realized STAR_T score.

In the graphic below, we provide a schematic overview of the counterfactual calculation.


Global plant locations
100-km search universe
100-km geodesic buffer
dissolve to one polygon
Erase ocean
Erase urban areas
Candidate region
66.86 million km^2 of land
Rasterise at 1 km
$\rightarrow$ 1 point per cell
Candidate points
66,861,619 points
Counterfactual sample
Solar: 16,330 units
Wind: 16,409 units
Candidate STAR/m^2
2.5-km geodesic buffer
Attach slope buildability
Solar: slope $\leq$ 5%
Wind: slope $\leq$ 20%
Within $d \in \{10, 20, 50, 100\}$ km
keep buildable candidate sites
Query minimum
STAR/m^2 among admissible sites
Multiply by plant area
and natural-land share $(1 - L_p)$
Counterfactual STAR$_T$ score
per plant, per radius

european corporate governance institute

about ECGI

The European Corporate Governance Institute has been established to improve *corporate governance through fostering independent scientific research and related activities.*

The ECGI will produce and disseminate high quality research while remaining close to the concerns and interests of corporate, financial and public policy makers. It will draw on the expertise of scholars from numerous countries and bring together a critical mass of expertise and interest to bear on this important subject.

The views expressed in this working paper are those of the authors, not those of the ECGI or its members.

www.ecgi.global

european corporate governance institute

ECGI Working Paper Series in Finance

Editorial Board

Editor	Nadya Malenko, Professor of Finance, Boston College
Consulting Editors	Renée Adams, Professor of Finance, University of Oxford Franklin Allen, Nippon Life Professor of Finance, Professor of Economics, The Wharton School of the University of Pennsylvania Julian Franks, Professor of Finance, London Business School Mireia Giné, Associate Professor, IESE Business School Marco Pagano, Professor of Economics, Facoltà di Economia Università di Napoli Federico II
Editorial Assistant	Asif Malik, Working Paper Series Manager

www.ecgi.global/content/working-papers

european corporate governance institute

Electronic Access to the Working Paper Series

The full set of ECGI working papers can be accessed through the Institute's Web-site (www.ecgi.global/content/working-papers) or SSRN:

Finance Paper Series	http://www.ssrn.com/link/ECGI-Fin.html
Law Paper Series	http://www.ssrn.com/link/ECGI-Law.html

www.ecgi.global/content/working-papers